











Article

Antispasmodic Effect of *Valeriana pilosa* Root Essential Oil and Potential Mechanisms of Action: Ex Vivo and In Silico Studies

Roberto O. Ybañez-Julca ^{1,*}, Ricardo Pino-Ríos ^{2,3}, Iván M. Quispe-Díaz ¹, Daniel Asunción-Alvarez ¹, Edwin E. Acuña-Tarrillo ¹, Elena Mantilla-Rodríguez ¹, Patricia Minchan-Herrera ¹, Marcelo A. Catalán ⁴, Liz Zevallos-Escobar ⁵, Edison Vásquez-Corales ⁵, Osvaldo Yáñez ⁶, Wilfredo O. Gutiérrez-Alvarado ⁷ and Julio Benites ^{2,3,*}

- ¹ Facultad de Farmacia y Bioquímica, Universidad Nacional de Trujillo, Trujillo 13011, Peru; iquispe@unitru.edu.pe (I.M.Q.-D.); hasuncion@unitru.edu.pe (D.A.-A.); eacunat@unitru.edu.pe (E.E.A.-T.); amantilla@unitru.edu.pe (E.M.-R.); pminchan@unitru.edu.pe (P.M.-H.)
- ² Química y Farmacia, Facultad de Ciencias de la Salud, Universidad Arturo Prat, Casilla 121, Iquique 1100000, Chile; rpinoiros@unap.cl
- ³ Instituto de Estudios de la Salud, Universidad Arturo Prat, Casilla 121, Iquique 1100000, Chile
- ⁴ Instituto de Fisiología, Facultad de Medicina, Universidad Austral de Chile, Valdivia 5090000, Chile; marcelo.catalan@uach.cl
- ⁵ Escuela de Farmacia y Bioquímica, Universidad Católica Los Ángeles de Chimbote, Chimbote 02801, Peru; lzevallose@uladech.edu.pe (L.Z.-E.); evasquezc@uladech.edu.pe (E.V.-C.)
- ⁶ Facultad de Ingeniería y Negocios, Universidad de las Américas, Santiago 7500000, Chile; oyanez@udla.cl
- ⁷ Facultad de Farmacia y Bioquímica, Universidad Nacional de la Amazonía Peruana, Iquitos 16001, Peru; wilfredo.gutierrez@unapiquitos.edu.pe
- * Correspondence: rybanez@unitru.edu.pe (R.O.Y.-J.); juliob@unap.cl (J.B.); Tel.: +51-0449-7634-5993 (R.O.Y.-J.); +56-57-2252-6275 (J.B.)



Citation: Ybañez-Julca, R.O.; Pino-Ríos, R.; Quispe-Díaz, I.M.; Asunción-Alvarez, D.; Acuña-Tarrillo, E.E.; Mantilla-Rodríguez, E.; Minchan-Herrera, P.; Catalán, M.A.; Zevallos-Escobar, L.; Vásquez-Corales, E.; et al. Antispasmodic Effect of *Valeriana pilosa* Root Essential Oil and Potential Mechanisms of Action: Ex Vivo and In Silico Studies. *Pharmaceutics* **2023**, *15*, 2072. <https://doi.org/10.3390/pharmaceutics15082072>

Academic Editor: Antonio Vassallo

Received: 18 July 2023

Revised: 28 July 2023

Accepted: 30 July 2023

Published: 2 August 2023



Copyright: © 2023 by the authors. Licensee MDPI, Basel, Switzerland. This article is an open access article distributed under the terms and conditions of the Creative Commons Attribution (CC BY) license (<https://creativecommons.org/licenses/by/4.0/>).

Abstract: Infusions of *Valeriana pilosa* are commonly used in Peruvian folk medicine for treating gastrointestinal disorders. This study aimed to investigate the spasmolytic and antispasmodic effects of *Valeriana pilosa* essential oil (VPEO) on rat ileum. The basal tone of ileal sections decreased in response to accumulative concentrations of VPEO. Moreover, ileal sections precontracted with acetylcholine (ACh), potassium chloride (KCl), or barium chloride (BaCl₂) were relaxed in response to VPEO by a mechanism that depended on atropine, hyoscine butylbromide, solifenacin, and verapamil, but not glibenclamide. The results showed that VPEO produced a relaxant effect by inhibiting muscarinic receptors and blocking calcium channels, with no apparent effect on the opening of potassium channels. In addition, molecular docking was employed to evaluate VPEO constituents that could inhibit intestinal contractile activity. The study showed that α -cubebene, β -patchoulene, β -bourbonene, β -caryophyllene, α -guaiene, γ -muurolene, valencene, eremophyllene, and δ -cadinene displayed the highest docking scores on muscarinic acetylcholine receptors and voltage-gated calcium channels, which may antagonize M₂ and/or M₃ muscarinic acetylcholine receptors and block voltage-gated calcium channels. In summary, VPEO has both spasmolytic and antispasmodic effects. It may block muscarinic receptors and calcium channels, thus providing a scientific basis for its traditional use for gastrointestinal disorders.

Keywords: *Valeriana pilosa*; antispasmodic effect; essential oil; molecular docking

1. Introduction

Gastrointestinal disorders are related to motility disturbances, visceral hypersensitivity, altered mucosal and immune functions, gut microbiota dysbiosis, and impaired regulation by the central nervous system [1]. Gastrointestinal dysfunction is associated with significant global healthcare costs [2,3] and decreased quality of life [4]. Existing synthetic antispasmodic drugs may cause unpleasant side effects such as dizziness, blurred

vision, fatigue, and dry mouth. Therefore, discovering new molecules with antispasmodic properties is an important goal for the pharmaceutical industry [5].

Medicinal plants are complex mixtures of compounds that have served as sources of drugs for centuries. Approximately half of the current pharmaceutical therapies are derived from medicinal plants [6].

Little is known about the effects of essential oils on the intestinal microbiota [7], which has been demonstrated to modulate intestinal motility [8–11]. Interestingly, short-chain fatty acids, mainly produced by intestinal bacteria, modulate intestinal motility [10].

Valeriana pilosa R & P. is a plant belonging to the genus *Valeriana* and distributed in the Andean region. In Peru, it is known as “Valeriana”, “Coche coche”, “Valeriana de paramo”, “Ornamo”, or “Babilla”. Vertical rhizome and attached roots from *Valeriana pilosa* are widely used as antispasmodic, relaxing, anti-inflammatory, and sleep-promoting agent [12,13].

Our continuous interest in the volatile components of plant species from Chilean and Peruvian Andean highland communities has been the focus of our chemical and biological research projects [14–19].

In this study, we report spasmolytic and antispasmodic activities of VPEO on intestinal contractile activity. The VPEO-mediated effect appears to be mediated by muscarinic receptor antagonism, calcium channel blockade, and potassium channel opening, which may explain the traditional use of the plant in gastrointestinal disorders. Additionally, we performed *in silico* molecular docking analyses of the major constituents in VPEO and found that some molecules have the potential to bind to M₂ muscarinic acetylcholine receptors (M₂R), M₃ muscarinic acetylcholine receptors (M₃R), and voltage-gated calcium channels (Ca_v1.2).

2. Materials and Methods

2.1. Chemicals, Drugs, and Solutions

Acetylcholine hydrochloride (ACh), barium chloride (BaCl₂), ethylenediaminetetraacetic acid (EDTA), calcium chloride (CaCl₂), glibenclamide, D-glucose, magnesium chloride (MgCl₂), potassium chloride (KCl), potassium dihydrogen phosphate (KH₂PO₄), sodium bicarbonate (NaHCO₃), sodium chloride (NaCl), sodium phosphate monobasic (NaH₂PO₄), and verapamil were purchased from Sigma-Aldrich (St. Louis, MO, USA) and Merck (Peruana S. A, Ate, Lima, Perú).

2.2. Plant Material

Roots (250 g) of *Valeriana pilosa* R & P. were collected in January 2022 in the Community of San Juan de Corralpampa at 3500 m above sea level, in the province of Hualgayoc, Department of Cajamarca, Perú. They were then subjected to hydrodistillation for 3 h, using a Clevenger-type apparatus. The oil obtained was dried over anhydrous sodium sulfate. Afterward, it was filtered and stored under protection at +4 °C for further analysis and testing [20].

2.3. Gas Chromatography Analysis (GC) and Gas Chromatography–Mass Spectrometry (GC–MS) of *Valeriana Pilosa* Essential Oil (VPEO)

All chemicals were of analytical reagent grade; they were obtained from Sigma-Aldrich-Fluka (St. Louis, MO, USA) and Merck (Darmstadt, Germany), and were used as supplied. Chromatographic analysis of VPEO was performed using a Perkin Elmer Clarus 600 gas chromatograph, following to the procedure reported by Benites et al. [19].

GC–MS analysis of VPEO was carried out as previously reported [20]. Briefly, analyses were performed on a Perkin Elmer Clarus 600 gas chromatograph, consisting of a DB-1 fused-silica column (30 m × 0.25 mm i.d., film thickness 0.25 µm; J & W Scientific, Folsom, CA, USA), and interfaced with a Perkin Elmer Clarus 600T mass spectrometer (software version 4.1, Perkin Elmer, Shelton, CT, USA). The injector and oven temperatures were as follows: transfer line temperature, 280 °C; ion source temperature, 220 °C; carrier gas, helium, adapted to a linear rate of 30 cm/s; split ratio, 1:40; ionization energy, 70 eV; scan

range, 40–300 m/z; and scan time, 1 s. The components were identified by comparing their retention indices relative to C₉–C₂₁ n-alkane indices and GC–MS spectra from the mass spectra library and commercial sample standards.

2.4. Animals

The experiments in this study were performed following the procedures of the American Veterinary Medical Association (AVMA) [21] and the Ethics Committee of Pharmacy and Biochemistry Faculty of the National University of Trujillo (COD.N^o: P 012-19/CEIFYB). Twenty male rats (8–10 weeks old *Rattus norvegicus* Holtzman, 170–200 g) were housed in cages (22–25 °C, 12 h light/dark cycles) with *ad libitum* access to standard rat chow (Molinorte S.A.C., Trujillo, Peru) and water.

2.5. Preparation of Rat Ileum

Animals were sacrificed by cervical dislocation. A portion of the ileum (2.5 cm), without considering the 10 cm nearest to the ileocecal valve, was removed and placed into a petri dish containing Tyrode's solution (concentrations in mM): NaCl 136.9; KCl 2.68; CaCl₂ 1.8; MgCl₂ 1.05; NaHCO₃ 11.9; NaH₂PO₄ 0.42; and D-glucose 5.55 [22]. Ileum fragments were placed into an isolated organ chamber filled with 25 mL of Tyrode's solution. The chamber was kept at 37 °C continuously gassed with a mixture of 95% O₂ and 5% CO₂ (pH 7.4). Resting tension was fixed at 1 g. The experimental data were recorded using a Power Lab 26T system (AD-Instruments Pty Ltd., Bella Vista, NSW, Australia) with the LabChart 8 program for Windows (Colorado Springs, CO, USA).

2.6. Ex Vivo Experimental Protocol

2.6.1. Effect of VPEO on the Basal Tone of Rat Ileum

The contractility of the rat ileum in response to VPEO was assessed through cumulative dose–response experiments. A series of seven distinct concentrations of VPEO (1, 10, 100, 250, 500, 750, and 1000 µg/mL) were administered in 5 min intervals [22].

2.6.2. Spasmolytic Effect in Precontracted Rat Ileum

Neurotropic spasm was induced using acetylcholine (ACh), whereas musculotropic spasm was induced using highly concentrated potassium chloride (KCl)- or barium chloride (BaCl₂)-containing solutions [22]. Isolated ileal sections were treated with ACh (10^{−5} M), KCl (60 mM), or BaCl₂ (5 mM) for 10 min or until a stable contractile plateau (plateau) was reached. Then, different VPEO concentrations (1, 10, 100, 250, 500, 750, and 1000 µg/mL) were sequentially added to the tissue chamber.

2.6.3. Antispasmodic VPEO Effect in the Dose–Response Curves of ACh, KCl, and BaCl₂

The effect of VPEO on the contractility in response to ACh was assessed as follows: dose–response experiments (ACh, 10^{−10} to 10^{−3} M) before and after VPEO (250 and 500 µg/mL) administration were performed in the same experiment.

Similar experiments to those described above but contracting the ileal sections with KCl (10^{−4} to 10^{−1} M) or BaCl₂ (10^{−8} to 10^{−2} M) were performed.

Dose–response data were fitted to the standard Hill's function using Graphpad.

2.6.4. Role of Extracellular Ca²⁺ Influx in the Intestinal VPEO-Mediated Relaxation

In addition to the Tyrode's solution, a calcium-free solution was prepared for this experiment. The solution had the following composition (concentrations in mM): KCl 50; NaCl 91.04; MgCl₂ 1.05; NaHCO₃ 11.87; NaH₂PO₄ 0.41; glucose 5.55; and EDTA 0.1 [23]. Initially, the tissue was stabilized in normal Tyrode's solution and then replaced with a Ca²⁺-free Tyrode's solution. Then, 10 min after the addition of calcium-free solution, the intestinal sections were contracted with ACh 10^{−5} M, followed by the addition of increasing CaCl₂ concentrations (0.1 mM; 0.3 mM; 0.6 mM; and 1 mM). Then, the tissue was washed

with normal Tyrode's solution for at least 10 min, followed by the addition of VPEO (250 and 500 µg/mL) for 20 min [22].

After VPEO incubation in normal Tyrode's solution, intestinal sections were incubated with VPEO-supplemented calcium-free solution, then contracted with ACh 10^{-5} M, followed by increasing CaCl₂ concentrations (0.1 mM; 0.3 mM; 0.6 mM, and 1 mM).

The tension was re-adjusted in the middle of the experiment to 1 g when necessary [22].

2.6.5. Effect of VPEO on Muscarinic Receptors

To analyze the role of VPEO in muscarinic receptor activity, experiments were carried out in the absence/presence of atropine (a non-selective muscarinic antagonist) [24], hyoscine butylbromide (M₂–M₃ blockers) [25], or solifenacin (selective M₃ blocker) [26]. First, the tissue was stabilized for 1 h and then washed in 15 min intervals (4–5 times) with Tyrode's solution. The tension was adjusted to 1 g when necessary. Then, ileal sections were treated with increasing doses of VPEO (1, 10, 100, 250, 500, 750, and 1000 µg/mL). Afterward, the sections were washed 4–5 times in 15 min intervals, and the tension was adjusted to 1 g. The tissue was pre-incubated for 20 min with 1.0 µM atropine, 1.0 µM hyoscine butylbromide, or 1.0 µM solifenacin, and then different VPEO concentrations were added (1–1000 µg/mL).

2.6.6. Effects of VPEO on Voltage-Gated Calcium Channel

To determine whether the effect of VPEO was related to the inhibition of voltage-gated calcium channel, experiments were performed in the absence and presence of verapamil (a voltage-gated calcium channel blocker). Initially, the tissue was stabilized for 1 h and then washed in 15 min intervals (4–5 times). The tension was adjusted again to 1 g if necessary. The tissue was pre-incubated with verapamil (1.0 µM) [27] for 20 min. Then, different VPEO concentrations (1, 10, 100, 250, 500, 750, and 1000 µg/mL) were added in intervals of 5 min.

2.6.7. Effects of VPEO on Potassium Channel Blockers

The role of K⁺ channels in VPEO-induced relaxation was investigated by pre-incubating the ileum rat for 20 min with two K⁺ channel blockers, namely, glibenclamide [28] (ATP sensitive K⁺ channel blocker), and barium chloride [29] (an inward rectifier K⁺ channel blocker). The tissue was stabilized for 1 h and then washed in 15 min intervals (4–5 times). The tension was adjusted again to 1 g if necessary. The tissue was pre-incubated with glibenclamide (10 µM) and barium chloride (1 mM) for 20 min. Then, VPEO was added (1, 10, 100, 250, 500, 750, and 1000 µg/mL) in intervals of 5 min for each successive dose, and the response was recorded.

2.7. *In Silico* Studies

Molecular modelling analysis of compounds 1–47 (see the SMILES in supplementary materials) of VPEO [20] to M₂ Muscarinic Acetylcholine Receptor [30], M₃ Muscarinic Acetylcholine Receptor [31], and Ca_v1.2 L-type voltage-gated calcium channel [32] were performed using AutoDock (v 4.2.1), AutoDock Vina (v 1.0.2) [33], and AutoDockTools packages [34]. The crystal structures considered for these docking studies had the following PDB Codes: 3UON (M₂ Muscarinic Acetylcholine Receptor), 4DAJ (M₃ Muscarinic Acetylcholine Receptor), and 5V2P (L-type voltage-gated calcium channel). Data was obtained from the Protein Data Bank [35]. The three-dimensional coordinates of all structures were optimized using MOPAC2016 software by the PM6-D3H4 semi-empirical method [36,37]. The crystal structures were treated with Schrödinger's Protein Preparation Wizard [38]; polar hydrogen atoms were added, nonpolar hydrogen atoms were merged, and charges were assigned. Docking was treated as rigid and performed using the empirical free energy function and Lamarckian Genetic Algorithm provided by AutoDock Vina [39]. The grid map dimensions were 20 × 20 × 20 Å³. The center of the binding site were the following coordinates for each of the proteins studied (Table 1).

Table 1. Cartesian coordinates of the center grid box (in Å) for M₂ Muscarinic Acetylcholine Receptor, M₃ Muscarinic Acetylcholine Receptor, and Ca_v1.2 (L-type voltage-gated calcium channel).

Protein	PDBID	Center Grid Box		
		x	y	z
M ₂ Muscarinic Acetylcholine Receptor	3UON	7.79	0.25	−3.95
M ₃ Muscarinic Acetylcholine Receptor	4DAJ	−14.79	−7.50	−42.53
Ca _v 1.2 L-type voltage-gated calcium channel	5V2P	7.76	42.10	123.95

All other parameters were set to their default values as defined by AutoDock Vina. Dockings were repeated 10 times, with the space search exhaustiveness set to 100. The best interaction binding energy (kcal·mol^{−1}) was selected for evaluation. Docking results in 3D representations were obtained using Discovery Studio [40] 3.1 (Accelrys, San Diego, CA, USA) molecular graphics system. The co-crystallized ligands were removed from their proteins and saved separately in the PDB format, which was used for redocking their respective protein active domains to validate our docking methodology [20].

Ligand Efficiency (LE), Binding Efficiency Index (BEI), Lipophilic Ligand Efficiency (LLE), and Non-Covalent Interaction Index (NCI) were calculated according to a previously reported procedure [20].

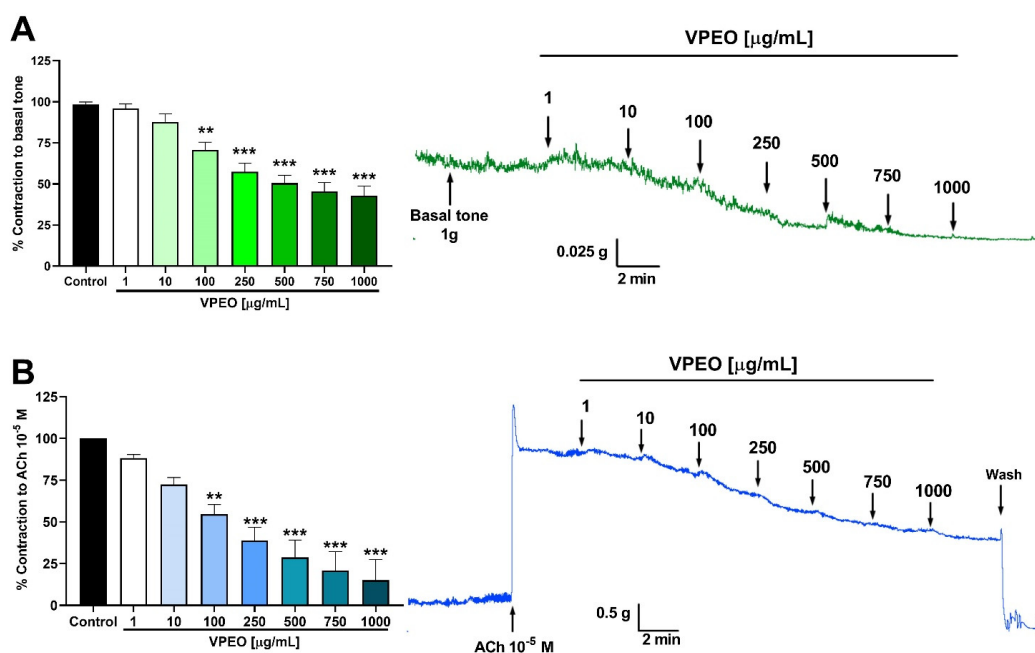
2.8. Statistical Analysis

GraphPad Prism 8.0.2 software (San Diego, CA, USA) was used for the statistical analyses. Non-linear regression analysis (three-parameter Hill function) was generated to compare dose–response curves. Two-way ANOVA analysis followed by the Bonferroni post hoc test was used to evaluate the significance between different groups.

3. Results

3.1. Spasmolytic Activity of VPEO on Rat Ileum

VPEO significantly decreased the muscle tone of the rat ileum at 100 µg/mL (70.63 ± 4.82% reduction compared to the control condition; *p* < 0.01) (Figure 1A). VPEO-mediated effect was dose-dependent, where 750 and 1000 µg/mL doses showed a higher effect compared to the 100 µg/mL dose (*p* < 0.05).

**Figure 1.** Cont.

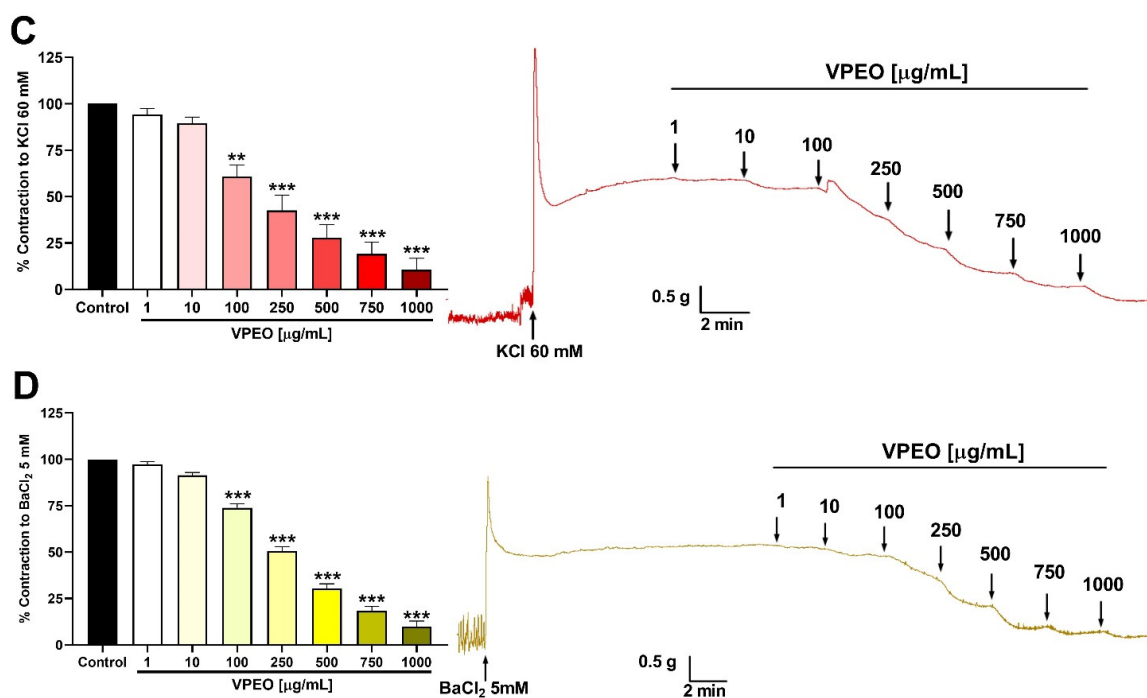


Figure 1. Effect of essential oil from *Valeriana pilosa* (VPEO) on rat ileum. VPEO relaxes the basal tone in rat ileum segments (A), VPEO-relaxed ileal segments precontracted with 10^{-5} M ACh (B), 60 mM KCl (C), or 5 mM BaCl₂ (D). In panel (A), the control represents the basal tone (100% contraction) without any treatment. In panels (B–D), the control represents the maximum response (100%) induced by ACh, KCl, and BaCl₂, respectively. In addition, original records of the relaxation effects of VPEO in the rat ileum are shown on the right side. Each bar represents the mean value of the response as a percentage \pm SEM of five experiments ($n = 5$). Statistical differences: ** $p < 0.01$; *** $p < 0.001$ vs. control.

The spasmolytic activity was determined by measuring the relaxation induced by VPEO in ileal sections precontracted with (a) 10^{-5} M ACh (muscarinic agonist) (Figure 1B), (b) 60 mM KCl (depolarizes the smooth muscle cell membrane and opens voltage-dependent Ca²⁺ channels) (Figure 1C), and (c) 5 mM BaCl₂ (a non-selective blocker of the current rectifying potassium channels; K_{IR}) (Figure 1D).

VPEO significantly relaxed, in a dose-dependent manner, precontracted intestinal segments with ACh, KCl, and BaCl₂. For instance, 100 $\mu\text{g/mL}$ VPEO relaxed ileal sections precontracted with ACh, KCl, and BaCl₂ by $54.62 \pm 5.7\%$, $60.88 \pm 6.2\%$, and $73.89 \pm 2.2\%$, respectively.

3.2. Antispasmodic Activity of VPEO on Rat Ileum

3.2.1. Role of Muscarinic Acetylcholine Receptors

Experiments were performed to determine whether VPEO modifies ACh-evoked intestinal contractions in the intact rat ileal tissue. Initially, ileum contractions were recorded before and after VPEO treatment (Figure 2A). VPEO at a dose of 500 $\mu\text{g/mL}$ significantly reduced ($p < 0.05$) the ACh-induced contraction (10^{-7} M ACh): $40.5 \pm 8.45\%$ (control) vs. $18.4 \pm 1.96\%$ (VPEO); Figure 2B,B.1. Similarly, in the presence of 1 μM atropine (a non-selective muscarinic receptor antagonist), the contractile effect of ACh (10^{-7} M) was suppressed ($4.6 \pm 1.19\%$, $p < 0.001$), as shown in Figure 2B.1. Moreover, increasing concentrations of ACh in the presence of VPEO significantly reduced ACh-induced contractions in the rat ileum (Figure 2B.1–B.4). Interestingly, in the Figure 2B, the nonlinear regression analysis of the dose–response curve shows that the pEC₅₀ values for ACh in the presence of 250 $\mu\text{g/mL}$ (6.22 ± 0.09) and 500 $\mu\text{g/mL}$ (5.75 ± 0.08) of VPEO were significantly different to that obtained under control conditions (6.53 ± 0.11).

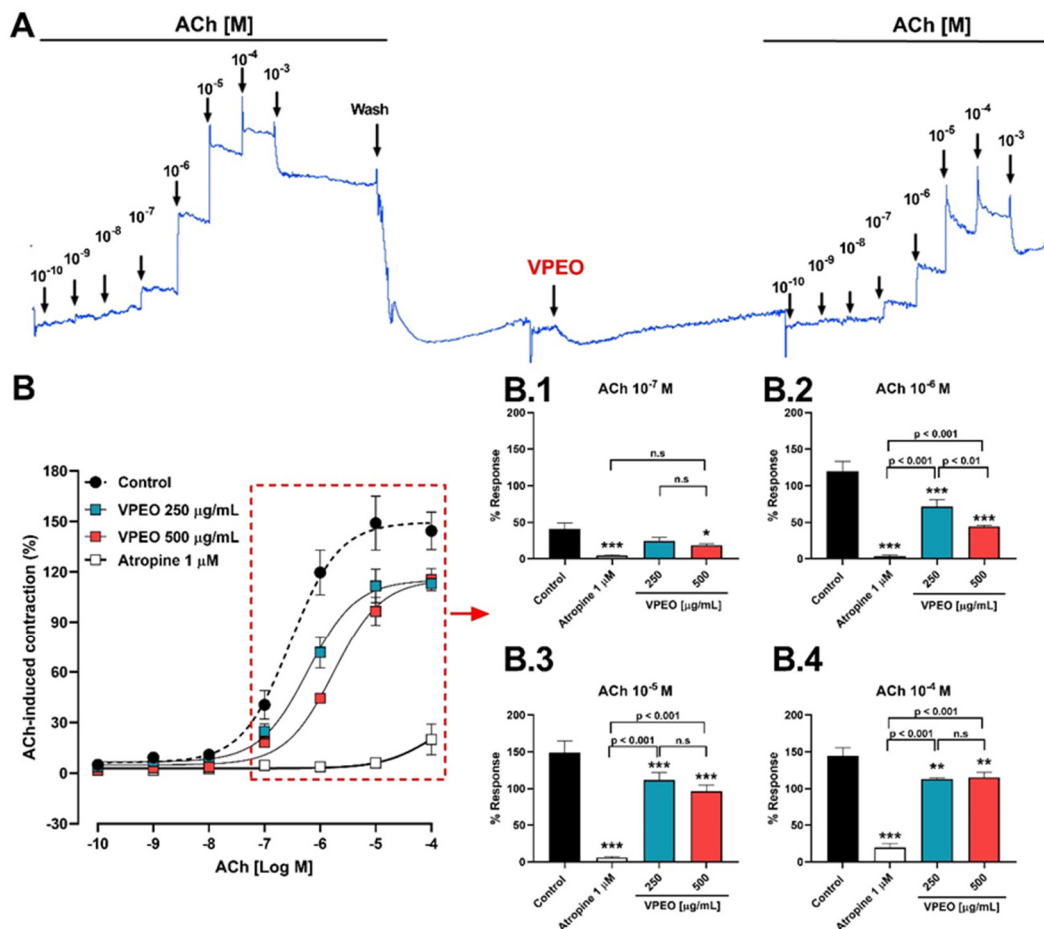


Figure 2. The antispasmodic activity of *Valeriana pilosa* essential oil (VPEO) reduces the contractile response to acetylcholine (ACh). The original record shows the effects of ACh on rat ileum segments in the absence and presence of VPEO. (A) The dose–response curve versus ACh when the rat ileum muscle tissue was pre-incubated with VPEO (250 and 500 μ g/mL) and atropine 1 μ M for 20 min before contraction with ACh. (B) Pre-incubation with VPEO (250 and 500 μ g/mL) and atropine 1 μ M reduced the contraction induced by ACh 10^{-7} – 10^{-4} M (B.1–B.4). Each point and bar represent the mean of maximal response in percentage \pm SEM of five experiments ($n = 5$). * $p < 0.05$; ** $p < 0.01$; *** $p < 0.001$ vs. control.

3.2.2. Effect of VPEO on Intestinal Sections Precontracted with KCl or BaCl₂

Figure 3A shows the effect of different KCl concentrations on ileum contractions. To study the antispasmodic activity, intestinal strips from wild-type rats were pre-incubated with the essential oil. VPEO significantly reduced the contraction induced by 10^{-2} M KCl: $71.46 \pm 8.93\%$ ($p < 0.05$) and $38.58 \pm 9.74\%$ ($p < 0.001$) compared to the control in the presence of 250 μ g/mL and 500 μ g/mL VPEO, respectively (Figure 3B.1). Similar results were observed for $10^{-1.5}$ M KCl: $62.82 \pm 6.03\%$ ($p < 0.01$) and $59.03 \pm 10.46\%$ ($p < 0.01$) compared to the control in the presence of 250 μ g/mL and 500 μ g/mL VPEO, respectively (Figure 3B.2). In Figure 3B, the nonlinear regression analysis of the dose–response curve shows that the sensitivity to KCl (pEC_{50}) in the presence of 250 μ g/mL (2.12 ± 0.25) and 500 μ g/mL (1.74 ± 0.29) VPEO was not significantly different from that obtained under control condition (2.19 ± 0.22).

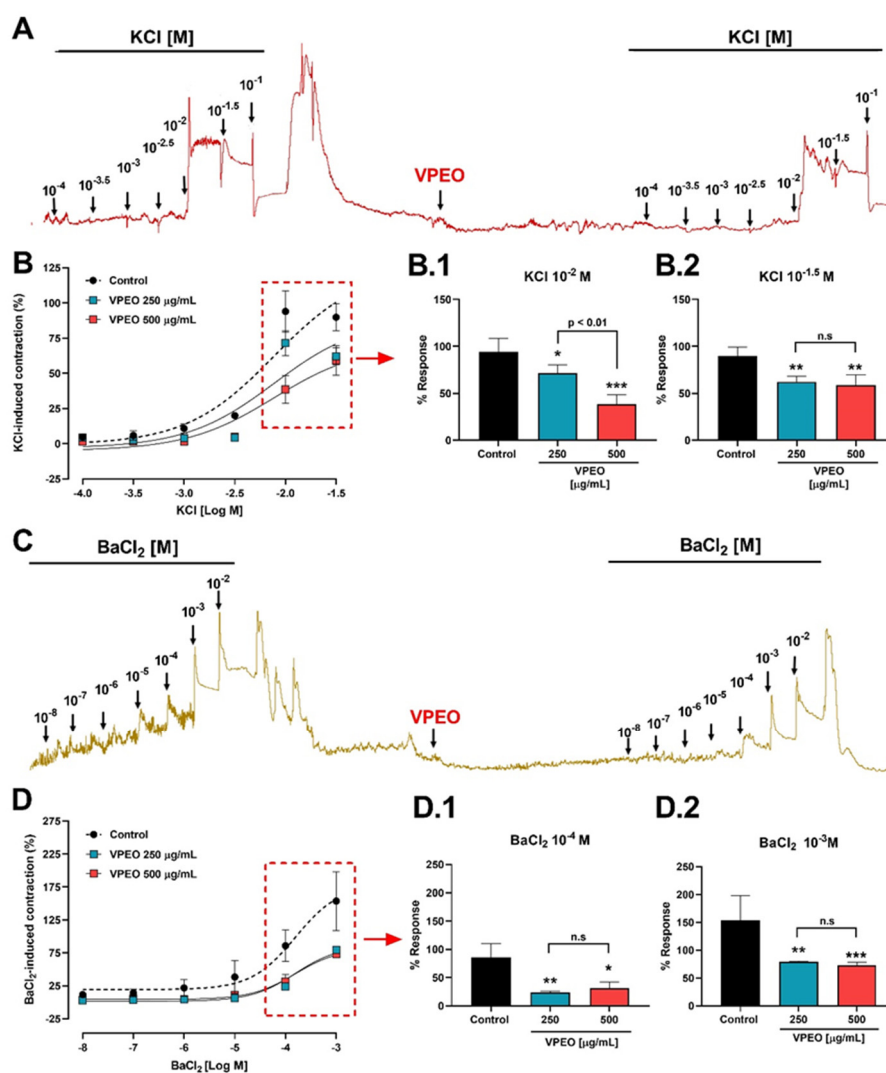


Figure 3. Antispasmodic activity of *Valeriana pilosa* essential oil (VPEO) in rat ileum. The original record shows the effects of KCl (A) and BaCl₂ (C) on rat ileum in the absence and presence of VPEO. Rat ileum muscle tissue was pre-incubated with VPEO (250 and 500 $\mu\text{g/mL}$) for 20 min before contraction with KCl (B) and BaCl₂ (D), and pre-incubation with VPEO 250 (B.1,D.1) and 500 $\mu\text{g/mL}$ (B.2,D.2) reduced contraction. Each point represents the mean of maximal response in percentage \pm SEM of five experiments ($n = 5$). n.s = not significant, statistical differences: * $p < 0.05$; ** $p < 0.01$; *** $p < 0.001$ vs. control.

On the other hand, high concentrations of BaCl₂ (10^{-8} – 10^{-2} M) block not only inward rectifier potassium channels (K_{IR}), but also voltage-gated potassium channels (VGKCs). In Figure 3C, the dose–response curves of ileum contractions induced by BaCl₂ in the presence and absence of VPEO are recorded. Pre-incubation with VPEO significantly reduced the contraction induced by 10^{-4} M BaCl₂: $23.75 \pm 2.47\%$ (250 $\mu\text{g/mL}$ VPEO; $p < 0.01$) and $31.18 \pm 11\%$ (500 $\mu\text{g/mL}$ VPEO; $p < 0.05$; Figure 3D.1); and 10^{-3} M BaCl₂: $79.5 \pm 1\%$ (250 $\mu\text{g/mL}$ VPEO; $p < 0.01$) and $73 \pm 5.2\%$ (500 $\mu\text{g/mL}$ VPEO; $p < 0.05$, Figure 3D.2) compared to the value obtained under control condition. In Figure 3D, the nonlinear regression analysis of the dose–response curve shows that the sensitivity to BaCl₂ (pEC_{50}) in the presence of 250 $\mu\text{g/mL}$ (3.35 ± 0.06) and 500 $\mu\text{g/mL}$ (3.68 ± 0.18) VPEO was not significantly different from that obtained under control condition (3.95 ± 0.36).

3.3. Determination of the Mechanisms of Action Underlying the VPEO Effect

3.3.1. Effect of VPEO on Muscarinic Receptors

After observing that VPEO reduced the effect of ileum contractions induced by ACh, we studied how VPEO affected the blockade of muscarinic receptors. The intestinal strips were pre-incubated with atropine (a non-selective muscarinic antagonist), hyoscine butylbromide (M_2 – M_3 muscarinic antagonist), and solifenacin (M_3 selective muscarinic antagonist), at doses of $1 \mu\text{M}$; then, concentrations of VPEO were added.

Figure 4A,B shows tissues pre-incubated with atropine and hyoscine butylbromide, respectively, at a dose of $1 \mu\text{M}$. In ileal tissues pre-incubated with $1 \mu\text{M}$ atropine (Figure 4A) or $1 \mu\text{M}$ hyoscine butylbromide (Figure 4B), the relaxant effect of $100 \mu\text{g}/\text{mL}$ VPEO was significantly ($p < 0.05$) reduced ($0.67 \pm 5.54\%$ and $0.63 \pm 10.55\%$) compared to ileal tissues that were not pre-incubated with antagonists ($29.37 \pm 4.82\%$). At the highest dose of VPEO ($1000 \mu\text{g}/\text{mL}$), the relaxation was more significant against atropine $1 \mu\text{M}$ ($18.33 \pm 7.67\%$, $p < 0.01$) than in hyoscine butylbromide $1 \mu\text{M}$ ($30 \pm 5.4\%$, $p < 0.05$) compared to the control ($57.15 \pm 5.84\%$). On the other hand, the relaxant dose–response of VPEO in the presence of solifenacin $1 \mu\text{M}$ decreased compared with that of the control, albeit not significantly ($p > 0.05$), as shown in Figure 4C.

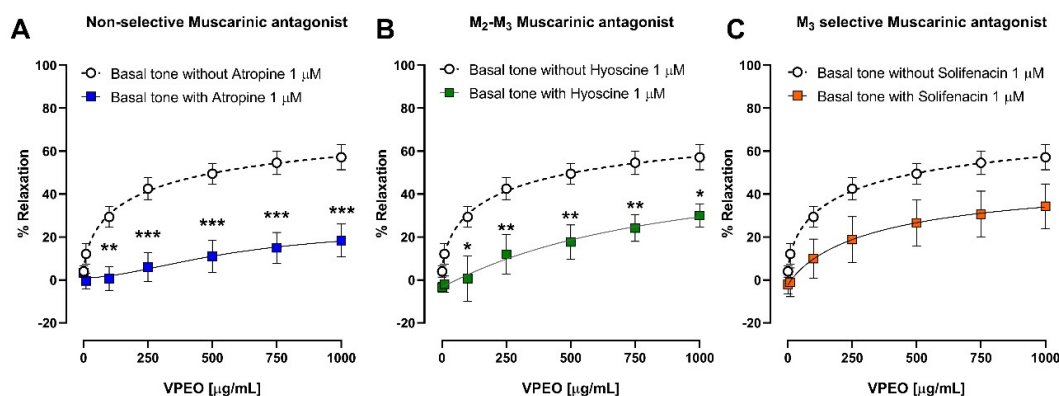


Figure 4. Relaxant effects of VPEO against (A) atropine $1 \mu\text{M}$, (B) Hyoscine butylbromide $1 \mu\text{M}$, (C) Solifenacin $1 \mu\text{M}$ in rat ileum sections. Each point represents the mean of maximal response in percentage \pm SEM of five experiments ($n = 5$). n.s. = not significant, statistical differences: * $p < 0.05$; ** $p < 0.01$; *** $p < 0.001$ vs. control.

These results indicate that the blockade of M_3 and M_2 receptors mediate the relaxant effect of VPEO.

3.3.2. Extracellular Ca^{2+} Dependence of VPEO Effect

The relation between the relaxant effect of VPEO (250 and $500 \mu\text{g}/\text{mL}$) and extracellular calcium was assessed. The contraction induced by the cumulative concentration of extracellular Ca^{2+} ions (0 to 1 mM) in ileum rats precontracted with ACh (10^{-5} M) maintained in Ca^{2+} -free Tyrode's solution (containing 0.1 mM EDTA) in the presence and absence of VPEO was determined (Figure 5A). The cumulative addition of calcium ions in Ca^{2+} -free Tyrode increased in the contraction of ileal sections in a concentration-dependent manner. Pre-treatment with VPEO at concentrations of $500 \mu\text{g}/\text{mL}$ ($171 \pm 29.1\%$ vs. 249.1 ± 23.8 control; $p < 0.01$) significantly decreased the contraction induced by CaCl_2 0.6 mM . However, the concentration–response curve produced by the different concentrations of calcium ions was significantly decreased in the presence of VPEO compared to the control (Figure 5B).

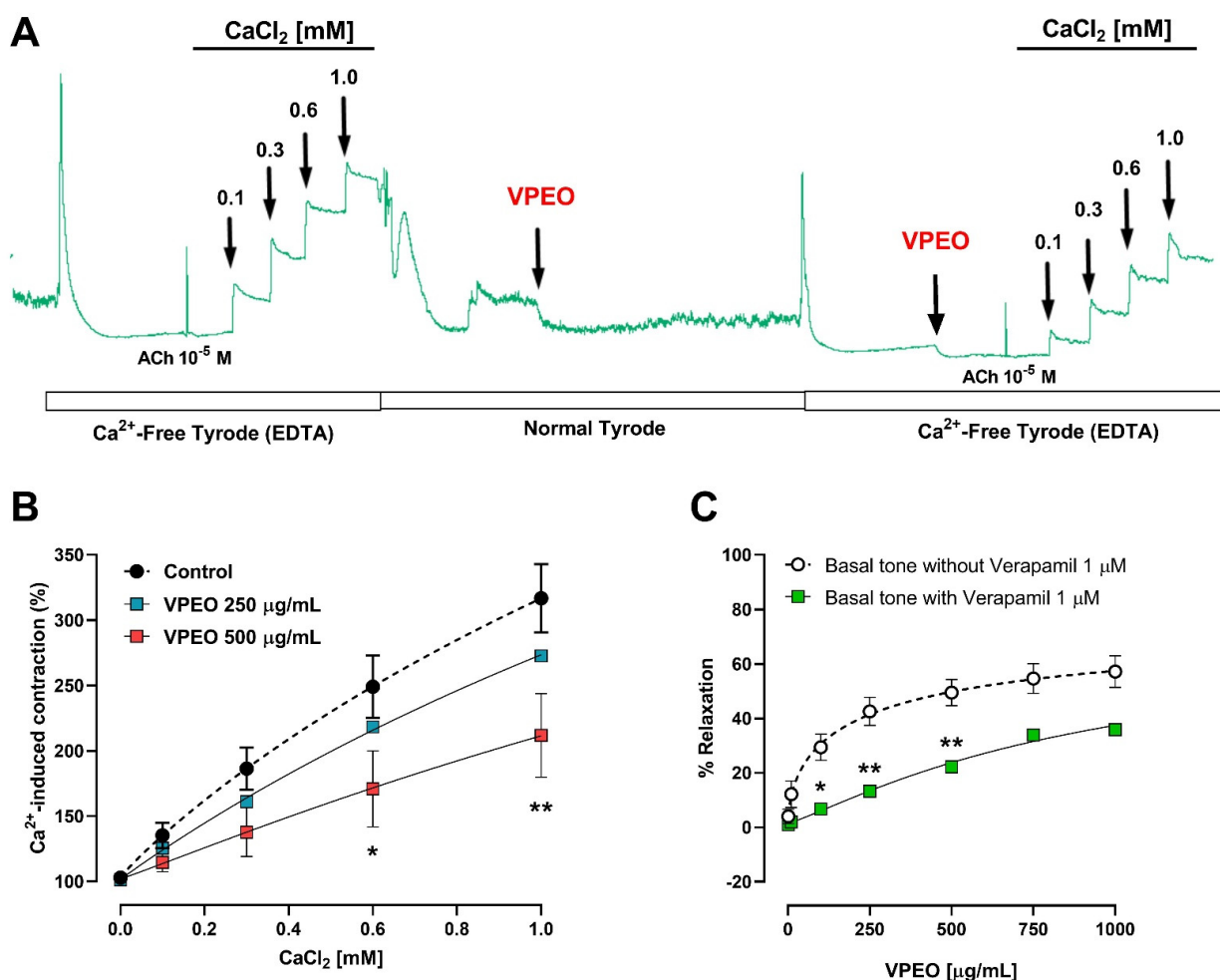


Figure 5. Effect of extracellular calcium in the presence and absence of VPEO in ileum rats precontracted with ACh (10^{-5} M). The original record shows the time course of the contractile response to CaCl_2 in Ca^{2+} -free Tyrode's solution (containing 0.1 mM EDTA) in the absence and presence of VPEO (A). Concentration-response curve of CaCl_2 in ileum rats in the absence and in the presence of VPEO (250 and 500 $\mu\text{g}/\text{mL}$) (B). Effects of verapamil (voltage-gated calcium channel blocker) on VPEO-induced relaxation in ileum rats (C). Each point represents the mean of maximal response in percentage \pm SEM ($n = 5-9$). * $p < 0.05$; ** $p < 0.01$ vs. control.

The relaxant effect produced by VPEO was decreased in the presence of verapamil 1 μM ($p < 0.05$, Figure 5C). For instance, relaxation induced by VPEO in ileal sections treated with 100 $\mu\text{g}/\text{mL}$ VPEO was 29.37 ± 4.82 vs. 6.73 ± 1.16 , control vs. verapamil, respectively. Taken together, the results suggest that essential oils might decrease contraction by reducing the entry of calcium ions into smooth muscle cells produced by extracellular calcium.

3.3.3. Effect of Two K^+ Channel Blockers on the Relaxation in Precontracted Ileum

The antispasmodic effect of VPEO in the rat ileum pre-incubated for 20 min with two K^+ channel blockers, glibenclamide (an ATP-sensitive K^+ channel blocker, 3 μM) and barium chloride (inward rectifier K^+ channel blocker, 1 mM) was studied. The relaxation induced by VPEO in the rat ileum was unaffected by glibenclamide (Figure 6A) or BaCl_2 (Figure 6B) treatment. Therefore, we conclude that *Valeriana pilosa* root essential oil does not induce opening of potassium channels in rat ileum.

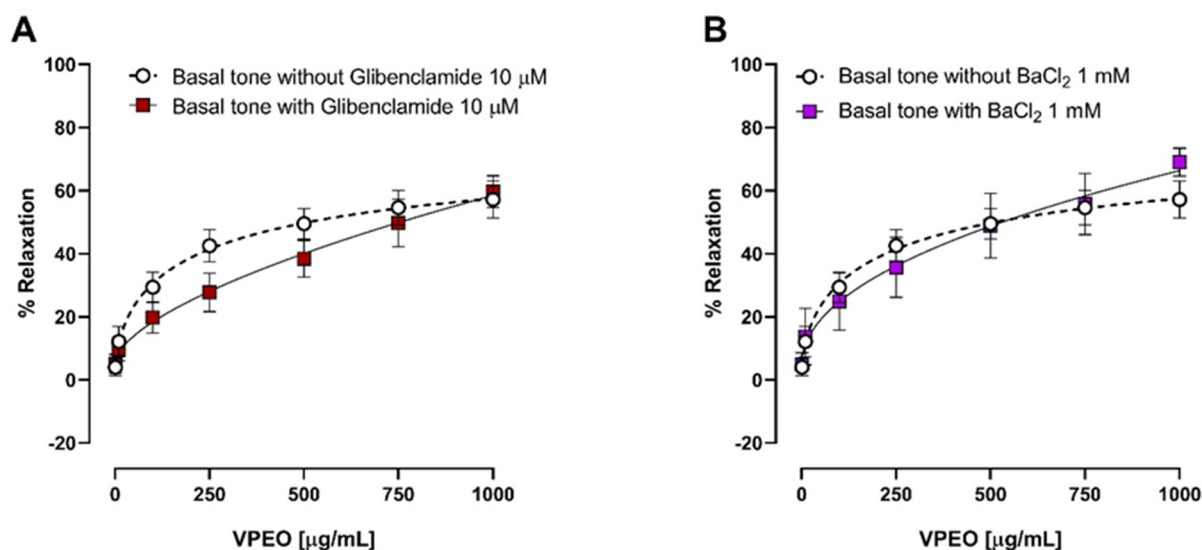


Figure 6. The effects of two potassium channel blockers separately of VPEO induced relaxation on rat ileum precontracted with KCl (20 mM) and ACh (10^{-5} M). (A) glibenclamide an ATP sensitive K^+ channel blocker, 10 μ M and (B) barium chloride, inward rectifier K^+ channel blocker, 1 mM. Data represented as mean \pm SEM (n = 4–8).

3.4. Molecular Docking and Ligand Efficiency Analysis of VPEO

We have recently described the chemical composition and antioxidant activity of the essential oil from *Valeriana pilosa* roots (VPEO). A total of 47 compounds were identified, where sesquiterpene hydrocarbons, monoterpene hydrocarbons, oxygenated monoterpenes, and oxygenated sesquiterpenes were the major constituents. Within the sesquiterpenes, the major constituents of VPEO were α -patchoulene (5.8%), α -humulene (6.1%), seychellene (7.6%), and patchoulol (20.8%), as well as spathulenol, T-cadinol, and γ -cadinol as minor constituents [20].

Molecular docking was performed to identify possible VPEO constituents that could inhibit some proteins involved in intestinal contractile activity. Based on the results obtained in the current study, we selected M_2 and M_3 Muscarinic Acetylcholine Receptor and $Ca_v1.2$ (L-type voltage-gated calcium channel). Table 2 shows a heat map of intermolecular docking energy values of 47 VPEO compounds. The values appear in a three-color scheme (red–yellow–green), where red represents the most stable binding energies and green represents the least stable ones. Table 2 shows a clear trend of compounds acting as putative inhibitors of the M_2 and M_3 muscarinic acetylcholine receptors.

Based on the information shown in Table 2, M_2 and M_3 muscarinic acetylcholine receptors appeared to be the best protein targets for some VPEO constituents, as shown by their intermolecular docking energy ($\Delta E_{binding}$), score normalization of the binding energy based on the number of non-hydrogen atoms ($IE_{norm.binding}$), and Ligand Efficiency (LE) values. Indeed, using the weighted arithmetic mean values (related to % of composition, see supplementary materials) shown in Table 3 obtained for all compounds, binding values were used for the analysis of M_2 muscarinic acetylcholine receptor: $\Delta E_{binding}$, LE, and $IE_{norm.binding}$ values were -7.67 , 0.55 , -2.06 kcal·mol $^{-1}$, and the M_3 muscarinic acetylcholine receptor, the $\Delta E_{binding}$, LE, and $IE_{norm.binding}$ were -8.03 , 0.58 , and -2.15 kcal·mol $^{-1}$, respectively, while, in comparison with the $Ca_v1.2$ (L-type voltage-gated calcium channel) protein target, the $\Delta E_{binding}$, LE, and $IE_{norm.binding}$, binding values were -5.11 , 0.37 , and -1.37 kcal·mol $^{-1}$. Therefore, these results show that the M_3 muscarinic acetylcholine receptor, as a target protein, is probably involved in the effects of VPEO, which means that they might be involved in the anti-spasmodic activities of VPEO compounds.

Table 2. Heat map of the intermolecular docking energy values (kcal·mol⁻¹) of VPEO compounds on M₂ and M₃ Muscarinic Acetylcholine and Ca_v1.2 (L-type VGCC) receptors.

N°	Components	M ₂	M ₃	Ca _v 1.2
1	Isovaleric acid	-4.8	-4.5	-4.2
2	Tricyclene	-6.8	-6.5	-4.4
3	α-Thujene	-6.5	-6.7	-4.6
4	α-Pinene	-6.5	-6.8	-4.3
5	Camphene	-6.9	-6.7	-4.6
6	3-Methyl valeric acid	-4.7	-4.8	-4.4
7	Sabinene	-6.5	-6.8	-4.7
8	1-Octen-3-ol	-5.2	-5.1	-3.7
9	β-Pinene	-6.6	-6.8	-4.4
10	Myrcene	-6	-5.9	-3.7
11	Limonene	-6.5	-6.5	-4.5
12	p-Cymene	-6.6	-6.5	-4.6
13	1,8-Cineole	-6.7	-6.7	-4.4
14	Linalool	-6	-5.9	-4.5
15	Isopentyl isovalerate	-5.8	-6.0	-4.3
16	Camphor	-6.9	-6.7	-4.2
17	Menthone	-6.9	-6.7	-4.4
18	Isomenthone	-6.9	-6.7	-4.4
19	Borneol	-6.8	-6.5	-4.1
20	Neomenthol	-6.8	-6.6	-4.2
21	Menthol	-6.4	-6.3	-4.2
22	Carvone	-6.9	-6.9	-4.7
23	Menthyl acetate	-7.5	-7.4	-4.7
24	α-Cubebene	-8.5	-9.0	-5.5
25	Cyclosativene	-8.5	-8.9	-5.4
26	α-Copaene	-8.2	-8.2	-5.3
27	β-Patchoulene	-9.1	-9.4	-5.8
28	β-Bourbonene	-8.9	-9.1	-5.1
29	β-Elemene	-8.1	-8.0	-5
30	β-Caryophyllene	-9.0	-9.1	-5.6
31	Seychellene	-7.9	-8.4	-5.4
32	α-Guaiene	-8.6	-9.0	-5.7
33	α-Humulene	-8.6	-9.1	-5.3
34	allo-Aromadendrene	-8.3	-8.6	-5.4
35	α-Patchoulene	-8.3	-8.7	-5.5
36	γ-Muurolene	-9.1	-9.2	-5.5
37	Germacrene-D	-8.6	-8.8	-5.2
38	Valencene	-8.5	-9.0	-5.6
39	Eremophyllene	-9.1	-8.9	-5.5
40	γ-Cadinene	-8.6	-8.6	-5.5
41	7-epi-α-Selinene	-8.3	-8.8	-5.4
42	δ-Cadinene	-8.8	-9.0	-5.4
43	Spathulenol	-8.6	-8.6	-5.4
44	β-Caryophyllene oxide	-8.1	-8.3	-5.5
45	T-Cadinol	-8.5	-8.8	-5.4
46	δ-Cadinol	-8.4	-8.8	-5.4
47	Patchoulol	-7.8	-8.6	-5.2

Values are listed as a three-colored scheme from red (high energy) to green (low energy).

Table 3. Average molecular docking results for the 47 compounds of VPEO regarding the M₂ and M₃ Muscarinic Acetylcholine Receptor and Ca_v1.2 (L-type VGCC). Intermolecular docking energy values ($\Delta E_{binding}$), Ligand Efficiency (LE), and normalizing binding energy ($IE_{norm.binding}$).

Proteins	$\bar{X}\Delta E_{binding}$ (kcal·mol ⁻¹)	$\bar{X}LE$ (kcal·mol ⁻¹)	$\bar{X}IE_{norm.binding}$ (kcal·mol ⁻¹)
M ₂ Muscarinic Acetylcholine Receptor	−7.67	0.55	−2.06
M ₃ M ₃ Muscarinic Acetylcholine Receptor	−8.03	0.58	−2.15
Ca _v 1.2 (L-type VGCC)	−5.11	0.37	−1.37

Molecular docking analyses, K_d values, Ligand Efficiency (LE), Binding Efficiency Index (BEI), Lipophilic Ligand Efficiency (LLE), and normalization of the binding energy score based on the number of non-hydrogen atoms ($IE_{norm.binding}$) are summarized in Table 4 for the top 12 (M₂ Muscarinic Acetylcholine Receptor) and 11 (M₃ Muscarinic Acetylcholine Receptor) compounds, of which the most abundant compounds found in the VPEO are presented. The results showed that approximately 60% of the VPEO compounds acted as potential blockers of M₂ and M₃ Muscarinic Acetylcholine Receptors. In contrast, the others showed higher values and were considered weak blockers with low activity for the other protein target Ca_v1.2 (L-type voltage-gated calcium channel).

Table 4. Molecular docking results from the best compounds of VPEO regarding the M₂ Muscarinic Acetylcholine Receptor and M₃ Muscarinic Acetylcholine Receptor with the major constituents of VPEO. Intermolecular docking energy values ($\Delta E_{binding}$), K_d values, Ligand Efficiency (LE), Binding Efficiency Index (BEI), Lipophilic Ligand Efficiency (LLE), and normalizing binding energy ($IE_{norm.binding}$) for the complexes.

N°	Components	$\Delta E_{binding}$ (kcal·mol ⁻¹)		K _d		LE (kcal·mol ⁻¹)		BEI (kDa)		LLE		$IE_{norm.binding}$ (kcal·mol ⁻¹)	
		M ₂	M ₃	M ₂	M ₃	M ₂	M ₃	M ₂	M ₃	M ₂	M ₃	M ₂	M ₃
24	α-Cubebene	−8.5	−9.0	5.90 × 10 ⁻⁷	2.54 × 10 ⁻⁷	0.60	0.60	30.5	32.3	2.0	2.3	−2.2	−2.3
27	β-Patchoulene	−9.1	−9.4	2.14 × 10 ⁻⁷	1.29 × 10 ⁻⁷	0.61	0.63	32.6	33.7	2.1	2.3	−2.3	−2.4
28	β-Bourbonene	−8.9	−9.1	3.00 × 10 ⁻⁷	2.14 × 10 ⁻⁷	0.59	0.61	31.9	32.6	2.3	2.4	−2.3	−2.3
30	β-Caryophyllene	−9.0	−9.1	2.54 × 10 ⁻⁷	2.14 × 10 ⁻⁷	0.60	0.61	32.0	32.3	1.8	1.9	−2.3	−2.3
31	Seychellene *	−7.9	−8.4	1.62 × 10 ⁻⁶	6.98 × 10 ⁻⁷	0.53	0.56	28.3	30.1	1.4	1.7	−2.0	−2.2
32	α-Guaiene	−8.6	−9.0	4.98 × 10 ⁻⁷	2.54 × 10 ⁻⁷	0.60	0.60	30.8	32.3	1.6	1.9	−2.2	−2.3
33	α-Humulene *	−8.6	−9.1	4.98 × 10 ⁻⁷	2.14 × 10 ⁻⁷	0.57	0.61	30.8	32.6	1.3	1.6	−2.2	−2.3
35	α-Patchoulene *	−8.3	−8.7	8.26 × 10 ⁻⁷	4.21 × 10 ⁻⁷	0.55	0.58	29.8	31.2	1.7	2.0	−2.1	−2.2
36	γ-Muurolene	−9.1	−9.2	2.14 × 10 ⁻⁷	1.81 × 10 ⁻⁷	0.61	0.61	32.6	33.0	2.1	2.2	−2.3	−2.4
38	Valencene	−8.5	−9.0	5.90 × 10 ⁻⁷	2.54 × 10 ⁻⁷	0.60	0.60	30.5	32.3	1.5	1.9	−2.2	−2.3
39	Eremophyllene	−9.1	−8.9	2.14 × 10 ⁻⁷	3.00 × 10 ⁻⁷	0.60	0.60	32.6	31.9	1.9	1.8	−2.3	−2.3
42	δ-Cadinene	−8.8	−9.0	3.55 × 10 ⁻⁷	2.54 × 10 ⁻⁷	0.60	0.60	31.6	32.3	1.7	1.9	−2.3	−2.3
47	Patchoulol *	−7.8	−8.6	1.92 × 10 ⁻⁶	4.98 × 10 ⁻⁷	0.49	0.54	25.7	28.3	2.1	2.7	−2.0	−2.2

* Represent the major constituents of the VPEO.

VPEO compounds obtained from molecular docking (see Table 4) displaying more binding potential to M₂ Muscarinic Acetylcholine Receptor were β-patchoulene, β-caryophyllene, γ-muurolene, and eremophyllene, while for the M₃ Muscarinic Receptor were α-cubebene, β-patchoulene, β-bourbonene, β-caryophyllene, α-guaiene, α-humulene, γ-muurolene, valencene, and δ-cadinene, all obtained $\Delta E_{binding}$ values (<−9.0) and $IE_{norm.binding}$ values (<−2.2), representing those with the highest interaction with residues close to the active site. In addition, the binding energies were evaluated for the major VPEO compounds, including natural sesquiterpenes such as α-patchoulene (5.8%), α-humulene (6.1%), seychellene (7.6%), and patchoulol (20.8%). (Detailed values of the interactions between individual compounds of the essential oil and the mentioned targets can be found supplementary materials)

Table 5 lists the non-covalent interactions present in the M₂-ligand complex. The four best compounds, β-patchoulene, β-caryophyllene, γ-muurolene, and eremophyllene,

identified by molecular docking presented weak Van der Waals-type and π -alkyl interactions (see Table 5 and Figure 7) with the binding site of M₂, where the most representative residues were Ala191, Ala194, Cys429, Phe181, Trp155, Trp400, Tyr104, and Tyr403. On the other hand, for the major VPEO compounds (see Table 5 and Figure 7), α -patchoulene, α -humulene, seychellene, and patchoulol had similar interactions of weak Van der Waals-type and π -alkyl interactions with the binding site of M₂, where the most representative residues of these interactions are Ala191, Ala194, Phe181, Trp155, Trp400, Tyr104, and Tyr403. However, patchoulol has a hydrogen bridge interaction between the hydroxyl group and Asn404, forming a favorable interaction in the binding of this compound by M₂.

Table 5. Amino acid residues of M₂ Muscarinic Acetylcholine Receptor (M₂R) and hydrogen bonding with the VPEO molecules within a distance of 3.5 Å.

Interacting Amino Acids in the Binding Pocket of M ₂ R	
Compound	Amino Acids (Distance in Å)
β -Patchoulene	Ala194 (5.43), Cys429 (4.53), Tyr104 (3.57), Phe195 (5.17), Trp400 (4.62), Tyr403 (3.77), Tyr426 (4.49).
β -Caryophyllene	Ala194 (3.83), Tyr104 (4.57), Trp155 (4.66), Trp400 (5.29), Tyr403 (4.51).
Seychellene *	Ala191 (4.22), Ala194 (4.77), Tyr104 (3.99), Trp155 (4.75), Phe181 (4.97), Trp400 (4.90), Tyr403 (4.86).
α -Humulene *	Ala194 (5.44), Tyr104 (4.80), Trp400 (5.20), Tyr403 (4.78).
α -Patchoulene *	Cys429 (5.17), Tyr104 (5.14), Phe181 (5.46), Trp400 (4.90), Tyr403 (5.38).
γ -Muuroolene	Ala191 (5.19), Ala194 (4.98), Cys429 (5.20), Tyr104 (5.04), Phe181 (4.80), Phe195 (5.25), Trp400 (5.20), Tyr403 (4.43), Tyr426 (4.70).
Eremophyllene	Val111 (5.15), Ala194 (3.92), Tyr104 (5.15), Trp155 (4.26), Trp400 (5.09), Tyr403 (4.12), Tyr426 (4.44).
Patchoulol *	Asn404 (2.08) **, Ala191 (3.97), Ala194 (4.31), Tyr104 (4.26), Trp155 (4.18), Phe195 (4.82), Trp400 (4.86), Tyr403 (4.90).

* Represent the major constituents of the VPEO. ** Represent H-bonds.

To extend the analysis, we focused on all possible protein–ligand interactions in the set of the best eight (identified by molecular docking) and the major VPEO compounds that interact with the M₃ Muscarinic Acetylcholine Receptor binding site (Table 6). These interactions define an interaction framework for the ligands in the analyzed set.

Table 6. Amino acid residues of M₃ Muscarinic Acetylcholine Receptor (M₃R) and hydrogen bonding with the VPEO molecules within a distance of 3.5 Å.

Interacting Amino Acids in the Binding Pocket of M ₃ R	
Compound	Amino Acids (Distance in Å)
α -Cubebene	Trp503 (3.65), Ala235 (4.43), Ala238 (4.30), Cys532 (3.89), Tyr148 (5.34), Trp199 (4.60), Trp503 (4.59), Tyr506 (4.85).
β -Patchoulene	Tyr506 (2.76), Ala238 (3.96), Cys532 (4.04), Tyr148 (3.64), Phe239 (5.47), Trp503 (4.39), Tyr506 (5.02).
β -Bourbonene	Ala235 (4.36), Ala238 (4.16), Cys532 (4.77), Tyr148 (5.22), Trp503 (5.24), Tyr506 (4.78).
β -Caryophyllene	Ala238 (4.70), Val155 (4.08), Tyr148 (5.18), Trp199 (4.23), Trp503 (4.88), Tyr506 (4.25), Tyr529 (5.34).
Seychellene *	Ala235 (4.08), Ala238 (3.79), Tyr148 (4.35), Trp199 (4.21), Trp503 (4.04), Tyr506 (4.77).
α -Guaiane	Trp503 (3.71), Ala235 (3.68), Ala238 (5.23), Cys532 (4.46), Val510 (4.30), Tyr148 (5.06), Trp199 (5.05), Trp503 (4.47), Tyr506 (4.23).
α -Humulene *	Ala235 (3.97), Cys532 (3.57), Val155 (4.38), Trp503 (3.59), Tyr506 (3.87), Tyr529 (4.68).
α -Patchoulene *	Tyr506 (2.57), Cys532 (4.03), Tyr148 (4.16), Trp503 (4.19), Tyr529 (4.19).
γ -Muuroolene	Cys532 (4.01), Tyr148 (3.73), Trp199 (5.01), Trp503 (4.31), Tyr506 (4.37), Tyr529 (4.69).
Valencene	Ala238 (3.94), Cys532 (4.43), Val155 (4.14), Tyr148 (4.10), Trp199 (4.40), Trp503 (5.17), Tyr506 (4.32), Tyr529 (4.76).
δ -Cadinene	Ala235 (3.67), Ala238 (4.65), Cys532 (3.62), Tyr148 (5.36), Trp199 (5.46), Trp503 (4.34), Tyr506 (5.01).
Patchoulol *	Asn507 (2.58) **, Ala235 (3.83), Ala238 (3.61), Tyr148 (4.54), Trp199 (4.64), Phe239 (5.23), Trp503 (4.40), Tyr506 (4.66).

* Represent the major constituents of the VPEO. ** Represent H-bonds.

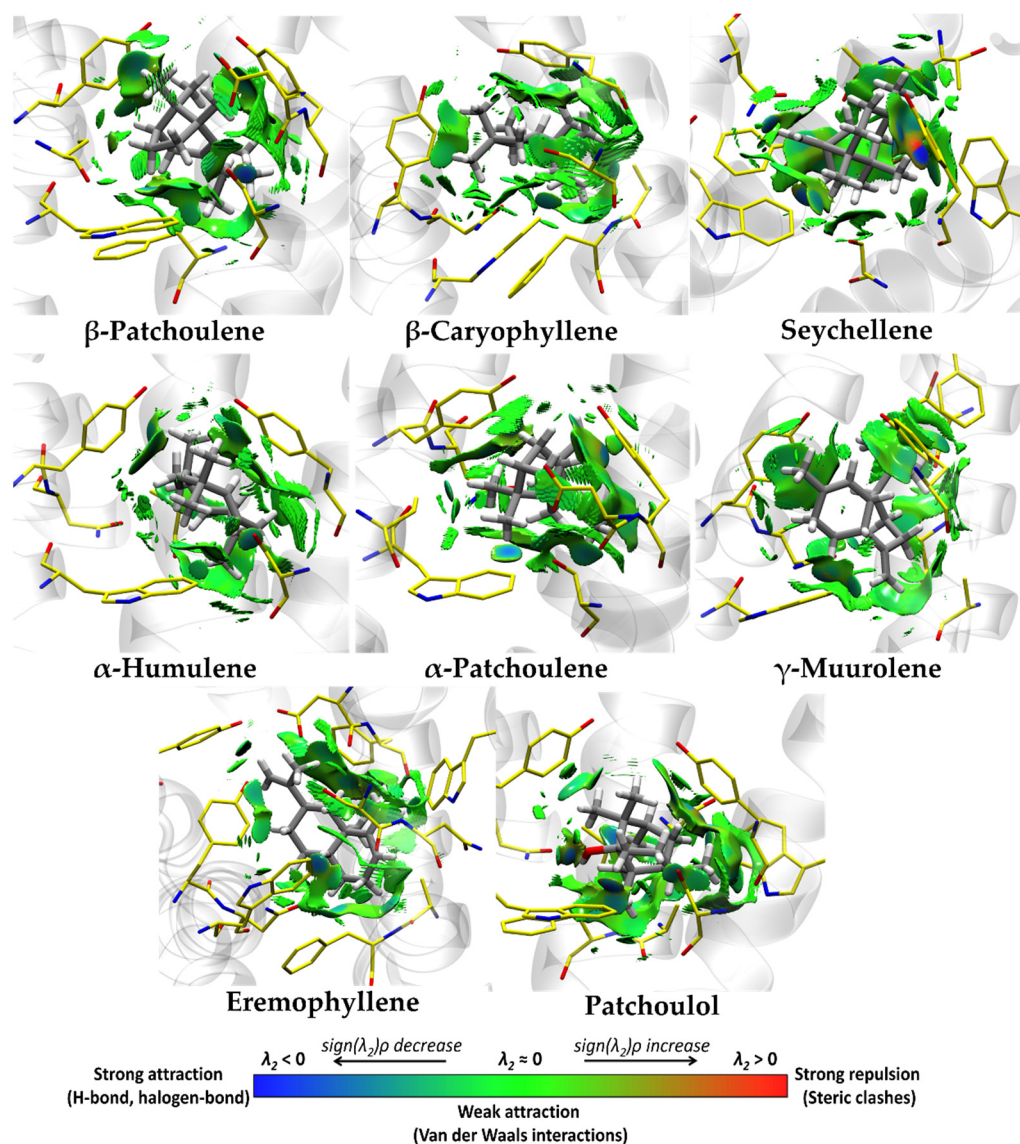


Figure 7. Non-covalent interactions analysis for the best four compounds (β -patchoulene, β -caryophyllene, γ -muurolele, and eremophyllene), and major constituents of the molecular docking of VPEO (α -patchoulene, α -humulene, seychellene, patchoulol) bound to M₂ muscarinic acetylcholine receptor.

Figure 8 shows the non-covalent interactions present in the M₃-ligand complex. The five best compounds, such as α -cubebene, β -patchoulene, β -bourbonene, β -caryophyllene, α -guaiene, γ -muurolele, valencene, and δ -cadinene, found by molecular docking present weak Van der Waals-type and π -alkyl interactions with the aromatic binding site of M₃, where the most representative residues are Tyr506, Tyr148, Phe239, Trp503, Tyr506, Trp199, and Tyr529. On the other hand, the major constituents of the VPEO as α -patchoulene, α -humulene, seychellene, and patchoulol, had similar interactions of weak Van der Waals-type and π -alkyl interactions with the aromatic binding site of M₃, where the most representative residues of these interactions are Ala235, Cys532, Val155, Trp503, Tyr506, and Tyr529. However, patchoulol has a hydrogen bridge interaction between the hydroxyl group and Asn507, favoring the potential binding of this compound to M₃.

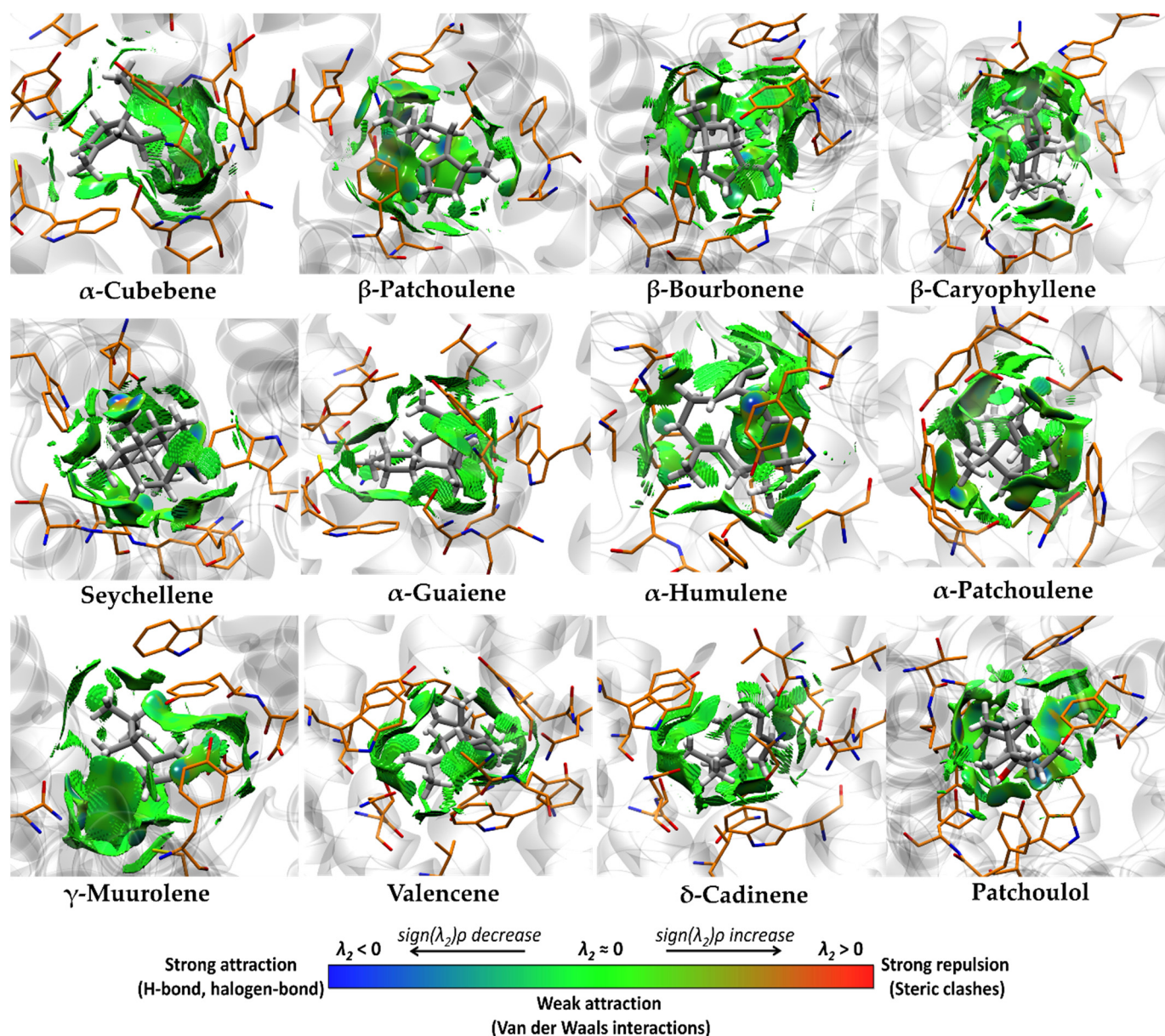


Figure 8. Non-covalent interactions analysis for the best nine compounds (α -cubebene, β -patchoulene, β -bourbonene, β -caryophyllene, α -guaiene, α -humulene, γ -muurolene, valencene, and δ -cadinene), and major (α -patchoulene, α -humulene, seychellene, patchoulol) constituents of the molecular docking of VPEO bound to M_3 muscarinic acetylcholine receptor.

4. Discussion

Essential oils are gaining interest due to their intricate chemical composition and diverse pharmacological effects. Among these actions, the antispasmodic effect is well known, although further research is required to better understand the cellular and molecular mechanisms of action [41]. Therefore, we studied the antispasmodic effect of *Valeriana pilosa* root essential oil (VPEO) and its underlying mechanisms of action using the isolated rat ileum ex vivo model. Our findings reveal that VPEO displays spasmolytic and antispasmodic effects in a dose-dependent manner at concentrations ranging from 100 to 1000 $\mu\text{g}/\text{mL}$. The relaxant activity of VPEO in the isolated rat ileum was reversible after washing, indicating that the inhibition observed was not attributable to intestinal damage caused by the oil's interaction with cell lipid bilayers [42].

Smooth muscle excitation and contraction in response to acetylcholine (ACh) release from autonomic nerves primarily involve the activation of muscarinic acetylcholine receptors (mAChRs) in the gastrointestinal tract and many other visceral organs [43]. The mAChR family comprises five molecularly distinct subtypes: M_1 – M_5 [44]. Smooth muscle mAChRs consist of M_2 and M_3 subtypes, with M_2 being predominant (M_2 : M_3 = 3–5:1) [43,45], although all five mAChR subtypes have been detected in the gastrointestinal smooth muscle at the mRNA level [46].

Activation of mAChRs triggers multiple biochemical and electrical signaling events that result in muscle contraction [47]. Our results demonstrated that VPEO, at a concentration of 250 $\mu\text{g}/\text{mL}$, reduced tonic contraction in ACh-precontracted tissues. Additionally, preincubation of intestinal tissues with VPEO (250 $\mu\text{g}/\text{mL}$) significantly reduced the pEC_{50} of the tissue to ACh, as evidenced by a rightward shift in the dose–response curve. These initial findings suggest that VPEO blocks muscarinic receptors involved in rat ileum contraction. To explore this hypothesis, we evaluated whether the presence of muscarinic antagonists such as atropine, hyoscine butylbromide, and solifenacin would attenuate the relaxing effect of VPEO. Our results showed that solifenacin, a selective blocker of M_3 muscarinic receptors, slightly reduced the relaxation induced by VPEO, but not significantly. In contrast, hyoscine butylbromide, an M_2 – M_3 muscarinic blocker, significantly reduced the relaxing effect of VPEO. Moreover, when the non-selective muscarinic blocker atropine was employed, the relaxing effect of VPEO on muscle tone in the rat ileum was further reduced. Traditional studies using various mAChR antagonists have suggested that the M_3 subtype primarily mediates contraction in visceral smooth muscles, while the contribution of the M_2 subtype remains less clear [48,49]. However, other investigations have demonstrated that the M_2 subtype modulates contraction, at least in part, by inhibiting cyclic AMP (cAMP)-dependent relaxation [43] and regulating smooth muscle ion channel activity [50–52]. Nevertheless, the precise mAChR subtype that mediates the contractile response remains largely unknown. Our findings indicate that, in addition to blocking M_3 receptors, the antispasmodic effect of VPEO also involves modulation of M_2 receptors. Consequently, both experimental and theoretical outcomes reveal the impact of VPEO on M_2 and M_3 muscarinic receptors.

There is limited research available on the effects of essential oils on cholinergic receptors expressed in smooth muscle, and a few studies have been published [6]. Molecular interactions between essential oil terpene compounds, such as vanillin, pulegone, eugenol, carvone, carvacrol, carveol, α -terpineol, thymol, thymoquinone, menthol, menthone, menthone, limonene, and nicotinic cholinergic receptors have been reported [53–55].

High concentrations of potassium ions (hypermolar KCl) cause tonic contraction of smooth intestinal muscles by a mechanism that depends on extracellular calcium influx [56,57]. Our study demonstrated that increasing concentrations of VPEO reduced contractions induced by 60 mM KCl. Additionally, when the tissue was pre-incubated for 20 min with the essential oil, the dose–response curves in response to KCl were significantly reduced. The action of VPEO can be attributed to its major component, patchouli alcohol (20.8%), a tricyclic sesquiterpene that has displayed similar results in other types of smooth muscle, such as the aorta [58] and rat corpus cavernosum [59]. However, the synergistic effects of other VPEO components, such as α -patchoulene (5.8%), α -humulene (6.1%), and seychellene (7.6%), at lower concentrations cannot be rejected.

Furthermore, it was confirmed that the relaxation induced by VPEO was reduced in the presence of verapamil, a voltage-gated calcium channel blocker. These results are consistent with similar studies conducted on the rhizome of *Valeriana hardwickii* Wall, which caused a rightward shift in calcium concentration–response curves in the rabbit jejunum, similar to that caused by verapamil [60,61]. The findings from our study on VPEO suggest the presence of an antispasmodic effect potentially mediated through calcium channel blockade.

It has been shown that ATP-sensitive potassium (K_{ATP}) channels regulate intestinal contractility [28]. These channels are heterooctameric proteins composed of pore-forming

subunits of the inwardly rectifying K^+ channel (K_{IR}) and subunits of the sulfonylurea regulatory receptor (SUR). The data demonstrate decreased intrinsic basal contractility in the small intestine and colon due to increased basal K_{ATP} channel activity, which can be inhibited by glibenclamide, an ATP-sensitive K^+ channel blocker [62], and $BaCl_2$, an inward rectifier K^+ channel blocker [63,64]. We observed that VPEO reduced $BaCl_2$ -induced contractions, shifting the dose–response curve to the right, suggesting that VPEO might activate K^+ channels, similar to the crude extract of *Valeriana wallichii*, which displays antispasmodic activity mediated by activation of the K_{ATP} channel [65]. To confirm these results, tissues were pre-incubated with glibenclamide and $BaCl_2$, and the relaxing effect of VPEO on basal tone was evaluated. Our results showed that the activation of K_{ATP} and K_{IR} channels did not produce the relaxation exhibited by VPEO in the rat ileum.

The monoterpene group, including compounds such as α -pinene, myrcene, limonene, *p*-cymene, 1,8-cineole, camphor, carvone, α -humulene, and spathulenol isolated from terrestrial plants, represents the chemical group with the highest number of antispasmodic compounds [66], which are also present in VPEO.

It is important to mention that several studies have shown that phytochemical analysis of essential oils from numerous plants can induce relaxation in smooth muscle across various animal species, which is often attributed to their antioxidant activity and ability to enhance gut and barrier function in animals [6,49,67]. Terpenes have been demonstrated to enhance gut microbiota, such as D-limonene [68,69], suggesting that this could be a possible explanation for how essential oils produce a calming effect on the gut.

In summary, our study provides experimental evidence showing antispasmodic properties of VPEO. Future in vivo experiments evaluating the effect of VPEO on the intestinal microbiota or determining optimal dosage are required to obtain more clues into the potential use of VPEO as a new pharmacological approach for treating muscle spasms.

5. Conclusions

The findings obtained from this study on *Valeriana pilosa* essential oil (VPEO) unequivocally demonstrated its spasmolytic and antispasmodic effects in rat ileum. In silico and pharmacological analyses suggest that VPEO exerts its actions through blockade of muscarinic receptors and calcium channels. Collectively, these outcomes provide molecular insights that shed light on the traditional utilization of this plant for the treatment of gastrointestinal disorders.

Supplementary Materials: The following supporting information can be downloaded at: <https://www.mdpi.com/article/10.3390/pharmaceutics15082072/s1>, Table S1. $\Delta E_{binding}$ (kcal·mol⁻¹), K_d , LE (kcal·mol⁻¹), BEI (kDa), LLE , $IE_{norm, binding}$ (kcal·mol⁻¹) obtained after molecular docking between *Valeriana pilosa* essential oil compounds and M₃ Muscarinic Acetylcholine Receptor (PDBID: 4DAJ). Table S2. $\Delta E_{binding}$ (kcal·mol⁻¹), K_d , LE (kcal·mol⁻¹), BEI (kDa), LLE , $IE_{norm, binding}$ (kcal·mol⁻¹) obtained after molecular docking between *Valeriana pilosa* essential oil compounds and M₂ Muscarinic Acetylcholine Receptor (PDBID: 3UON). Table S3. $\Delta E_{binding}$ (kcal·mol⁻¹), K_d , LE (kcal·mol⁻¹), BEI (kDa), LLE , $IE_{norm, binding}$ (kcal·mol⁻¹) obtained after molecular docking between *Valeriana pilosa* essential oil compounds and L-type voltage-gated calcium channel (PDBID: 5V2P). Table S4. Percentage composition of the essential oil isolated from *Valeriana pilosa*. Table S5. Smiles for all compounds in *Valeriana pilosa* essential oil.

Author Contributions: Conceptualization, R.O.Y.-J., O.Y. and J.B.; methodology, D.A.-A., I.M.Q.-D., R.O.Y.-J., O.Y. and J.B.; formal analysis, D.A.-A., R.O.Y.-J., I.M.Q.-D. and E.M.-R.; investigation, P.M.-H., E.E.A.-T., W.O.G.-A., L.Z.-E., E.V.-C., O.Y., R.P.-R. and J.B.; writing—original draft preparation, R.O.Y.-J., M.A.C. and J.B.; writing—review and editing, M.A.C. and J.B.; funding acquisition, R.O.Y.-J. and J.B. All authors have read and agreed to the published version of the manuscript.

Funding: This research was funded by Proyecto Canon Minero (R.R. N° 0262–2021/UNT, Perú), and Fondo Interno VRII-UNAP, grant number (VRIIP0056-21, Chile).

Institutional Review Board Statement: Not applicable.

Informed Consent Statement: Not applicable.

Data Availability Statement: Not applicable.

Conflicts of Interest: The authors declare no conflict of interest.

References

1. Drossman, D.A. History of functional gastrointestinal symptoms and disorders and chronicle of the Rome Foundation. In *Rome IV Functional Gastrointestinal Disorders: Disorders of Gut-Brain Interaction*; Drossman, D.A., Chang, L.C., Kellow, W.J., Tack, J., Whitehead, W.E., Eds.; The Rome Foundation: Raleigh, NC, USA, 2016; pp. 549–576.
2. Canavan, C.; West, J.; Card, T. Review article: The economic impact of the irritable bowel syndrome. *Aliment. Pharmacol. Ther.* **2014**, *40*, 1023–1034. [[CrossRef](#)]
3. Tack, J.; Stanghellini, V.; Mearin, F.; Yiannakou, Y.; Layer, P.; Coffin, B.; Simren, M.; Mackinnon, J.; Wiseman, G.; Marciniak, A.; et al. Economic burden of moderate to severe irritable bowel syndrome with constipation in six European countries. *BMC Gastroenterol.* **2019**, *19*, 69–82. [[CrossRef](#)]
4. Wong, R.K.; Drossman, D.A. Quality of life measures in irritable bowel syndrome. *Expert Rev. Gastroenterol. Hepatol.* **2010**, *4*, 277–284. [[CrossRef](#)]
5. Clark, A.M. Natural products as a resource for new drugs. *Pharm. Res.* **1996**, *13*, 1133–1141. [[CrossRef](#)] [[PubMed](#)]
6. Heghes, S.C.; Vostinaru, O.; Rus, L.M.; Mogosan, C.; Iuga, C.A.; Filip, L. Antispasmodic Effect of Essential Oils and Their Constituents: A Review. *Molecules* **2019**, *24*, 1675. [[CrossRef](#)] [[PubMed](#)]
7. Lazar, V.; Holban, A.M.; Curutiu, C.; Ditu, L.M. Modulation of Gut Microbiota by Essential Oils and Inorganic Nanoparticles: Impact in Nutrition and Health. *Front. Nutr.* **2022**, *9*, 920413. [[CrossRef](#)]
8. Waclawiková, B.; Bullock, A.; Schwalbe, M.; Aranzamendi, C.; Nelemans, S.A.; van Dijk, G.; El Aidy, S. Gut bacteria-derived 5-hydroxyindole is a potent stimulant of intestinal motility via its action on L-type calcium channels. *PLoS Biol.* **2021**, *19*, e3001070. [[CrossRef](#)]
9. Kang, S.; Park, M.Y.; Brooks, I.; Lee, J.; Kim, S.H.; Kim, J.Y.; Oh, B.; Kim, J.W.; Kwon, O. Spore-forming *Bacillus coagulans* SNZ 1969 improved intestinal motility and constipation perception mediated by microbial alterations in healthy adults with mild intermittent constipation: A randomized controlled trial. *Food Res. Int.* **2021**, *146*, 110428. [[CrossRef](#)]
10. Blakeney, B.A.; Crowe, M.S.; Mahavadi, S.; Murthy, K.S.; Grider, J.R. Branched short-chain fatty acid isovaleric acid causes colonic smooth muscle relaxation via cAMP/PKA pathway. *Dig. Dis. Sci.* **2019**, *64*, 1171–1181. [[CrossRef](#)] [[PubMed](#)]
11. Waclawiková, B.; Codutti, A.; Alim, K.; El Aidy, S. Gut microbiota-motility interregulation: Insights from in vivo, ex vivo and in silico studies. *Gut Microbes* **2022**, *14*, 1997296. [[CrossRef](#)] [[PubMed](#)]
12. Galan, A.; Sanchez, I.; Montoya, J.; Linares, E.; Campos, J.; Vicente, J. La vegetación del norte del Perú: De los bosques a la jalca en Cajamarca. *Acta Bot. Malac.* **2015**, *40*, 157–190. [[CrossRef](#)]
13. Seminario-Cunya, J.; Rumay-Sanchez, L.; Seminario-Cunya, A. Biología de Valeriana pilosa R. & P. (Valerianaceae): Una especie en peligro de extinción de las altas montañas de Perú. *Bol. Latinoam. Caribe Plants Med. Aromat.* **2016**, *15*, 337–351.
14. Rojo, L.; Benites, J.; Rodriguez, A.; Venancio, F.; Ramalho, L.; Teixeira, A.; Feio, S.; do Ceu Costa, M. Composition and antimicrobial screening of the essential oil of *Acantholippia deserticola* (Phil.ex F. Phil.) Moldenke. *J. Essent. Oil Res.* **2006**, *18*, 695–697. [[CrossRef](#)]
15. Rojo, L.E.; Benites, J.; López, J.; Rojas, M.; Díaz, P.; Pastene, E.; Ordoñez, J. Comparative study on the antioxidant effects and phenolic content of twelve highly consumed medicinal plants from South American Andes. *Bol. Latinoam. Caribe Plants Med. Aromat.* **2009**, *8*, 498–508.
16. Benites, J.; Moiteiro, C.; Miguel, G.; Rojo, L.; López, J.; Venancio, F.; Ramalho, L.; Feio, S.; Dandlen, S.; Casanova, H.; et al. Composition and biological activity of the essential oil of Peruvian Lantana camara. *J. Chil. Chem. Soc.* **2009**, *54*, 379–384. [[CrossRef](#)]
17. Benites, J.; López, J.; Rojo, L.; Díaz, P.; Rojas, M.; Venancio, F.; Moiteiro, M. Chemical composition of the essential oil of the leaves and stems of *Xenophyllum poposum*. *Chem. Nat. Compound.* **2011**, *46*, 988–989. [[CrossRef](#)]
18. Benites, J.; Moiteiro, C.; Figueiredo, A.C.; Rijo, P.; Buc-Calderon, P.; Bravo, F.; Gajardo, S.; Sánchez, I.; Torres, I.; Ganoza, M. Chemical composition and antimicrobial activity of essential oil of Peruvian Dalea strobilacea Barneby. *Bol. Latinoam. Caribe Plants Med. Aromat.* **2016**, *15*, 429–435.
19. Benites, J.; Ríos, D.; Guerrero-Castilla, A.; Enríquez, C.; Zavala, E.; Ybañez-Julca, R.O.; Quispe-Díaz, I.; Jara-Aguilar, R.; Buc Calderon, P. Chemical Composition and Assessment of Antimicrobial, Antioxidant and Antiproliferative Activities of Essential oil from *Clinopodium sericeum*, a Peruvian Medicinal Plant. *Rec. Nat. Prod.* **2021**, *15*, 175–186. [[CrossRef](#)]
20. Minchán-Herrera, P.; Ybañez-Julca, R.O.; Quispe-Díaz, I.M.; Venegas-Casanova, E.A.; Jara-Aguilar, R.; Salas, F.; Zevallos-Escobar, L.; Yáñez, O.; Pino-Rios, R.; Buc Calderon, P.; et al. Valeriana pilosa Roots Essential Oil: Chemical Composition, Antioxidant Activities and Molecular Docking Studies on Enzymes involved in Redox Biological Processes. *Antioxidants* **2022**, *11*, 1337. [[CrossRef](#)]
21. AVMA (American Veterinary Medical Association). *AVMA Guidelines for the Euthanasia of Animals*, 2020 ed.; AMVA: Schaumburg, IL, USA, 2020. Available online: <https://www.avma.org/KB/Policies/Documents/euthanasia.pdf> (accessed on 26 March 2021).
22. Ybañez-Julca, R.O.; Asunción-Alvarez, D.; Quispe-Díaz, I.M.; Palacios, J.; Bórquez, J.; Simirgiotis, M.J.; Perveen, S.; Nwokocha, C.R.; Cifuentes, F.; Paredes, A. Metabolomic Profiling of Mango (*Mangifera indica* Linn) Leaf Extract and Its Intestinal Protective Effect and Antioxidant Activity in Different Biological Models. *Molecules* **2020**, *25*, 5149. [[CrossRef](#)] [[PubMed](#)]

23. Hassan Gilani, A.U.; Aziz, N.; Ahmad, M.; Alam, M.T.; Rizwani, G.H. Spasmogenic and Spasimolytic Constituents in Sida Pakistanica. *Pharm. Biol.* **1999**, *37*, 173–180. [[CrossRef](#)]
24. Ryoo, S.B.; Oh, H.K.; Moon, S.H.; Choe, E.K.; Yu, S.A.; Park, S.H.; Park, K.J. Electrophysiological and Mechanical Characteristics in Human Ileal Motility: Recordings of Slow Waves Conductions and Contractions, In Vitro. *Korean J. Physiol. Pharmacol.* **2015**, *19*, 533–542. [[CrossRef](#)] [[PubMed](#)]
25. Zhang, L.; Song, J.; Bai, T.; Lu, X.; Yang, G.; Qian, W.; Wang, R.; Hou, X. Effects of Buscopan on Human Gastrointestinal Smooth Muscle Activity in an Ex Vivo Model: Are There Any Differences for Various Sections? *Eur. J. Pharmacol.* **2016**, *780*, 180–187. [[CrossRef](#)]
26. Veer, V.; Chess-Williams, R.; Moro, C. Antimuscarinic Actions on Bladder Urothelium and Lamina Propria Contractions Are Similar to Those Observed in Detrusor Smooth Muscle Preparations. *Neurourol. Urodyn.* **2023**, *42*, 1080–1087. [[CrossRef](#)] [[PubMed](#)]
27. Gaion, R.M.; Trento, M. Prostacyclin-Induced Contraction of Guinea-Pig Ileum: Influence of Drugs Affecting Calcium Flux in the Smooth Muscle. *Eur. J. Pharmacol.* **1984**, *102*, 529–533. [[CrossRef](#)] [[PubMed](#)]
28. York, N.W.; Parker, H.; Xie, Z.; Tyus, D.; Waheed, M.A.; Yan, Z.; Grange, D.K.; Remedi, M.S.; England, S.K.; Hu, H.; et al. Kir6.1- and SUR2-Dependent KATP Overactivity Disrupts Intestinal Motility in Murine Models of Cantú Syndrome. *JCI Insight* **2020**, *5*, e141443. [[CrossRef](#)] [[PubMed](#)]
29. Krapivinsky, G.; Medina, I.; Eng, L.; Krapivinsky, L.; Yang, Y.; Clapham, D.E. A Novel Inward Rectifier K⁺ Channel with Unique Pore Properties. *Neuron* **1998**, *20*, 995–1005. [[CrossRef](#)]
30. Haga, K.; Kruse, A.C.; Asada, H.; Yurugi-Kobayashi, T.; Shiroishi, M.; Zhang, C.; Weis, W.I.; Okada, T.; Kobilka, B.K.; Haga, T.; et al. Structure of the human M2 muscarinic acetylcholine receptor bound to an antagonist. *Nature* **2012**, *482*, 547–551. [[CrossRef](#)]
31. Kruse, A.C.; Hu, J.; Pan, A.C.; Arlow, D.H.; Rosenbaum, D.M.; Rosemond, E.; Green, H.F.; Liu, T.; Chae, P.S.; Dror, R.O.; et al. Structure and dynamics of the M3 muscarinic acetylcholine receptor. *Nature* **2012**, *482*, 552–556. [[CrossRef](#)]
32. Findeisen, F.; Campiglio, M.; Jo, H.; Abderemane-Ali, F.; Rumpf, C.H.; Pope, L.; Rossen, N.D.; Flucher, B.E.; DeGrado, W.F.; Minor, D.L., Jr. Stapled Voltage-Gated Calcium Channel (Ca_v) α -Interaction Domain (AID) Peptides Act As Selective Protein-Protein Interaction Inhibitors of Ca_v Function. *ACS Chem. Neurosci.* **2017**, *8*, 1313–1326. [[CrossRef](#)] [[PubMed](#)]
33. Trott, O.; Olson, A. AutoDock Vina: Improving the speed and accuracy of docking with a new scoring function, efficient optimization and multithreading. *J. Comput. Chem.* **2010**, *31*, 455–461. [[CrossRef](#)]
34. Sanner, M.F. Python: A programming language for software integration and development. *J. Mol. Graph. Model.* **1999**, *17*, 55–84. [[CrossRef](#)]
35. Berman, H.M.; Westbrook, J.; Feng, Z.; Gilliland, G.; Bhat, T.N.; Weissig, H.; Shindyalov, I.N.; Bourne, P.E. The Protein Data Bank. *Nucleic Acids Res.* **2000**, *28*, 235–242. [[CrossRef](#)]
36. Stewart, J.J.P. Optimization of parameters for semiempirical methods V: Modification of NDDO approximations and application to 70 elements. *J. Mol. Model.* **2007**, *13*, 1173–1213. [[CrossRef](#)] [[PubMed](#)]
37. Řezáč, J.; Hobza, P. Advanced corrections of hydrogen bonding and dispersion for semiempirical quantum mechanical methods. *J. Chem. Theory Comput.* **2012**, *8*, 141–151. [[CrossRef](#)]
38. Madhavi Sastry, G.; Adzhigirey, M.; Day, T.; Annabhimoju, R.; Sherman, W. Protein and ligand preparation: Parameters, protocols, and influence on virtual screening enrichments. *J. Comput. Aided Mol. Des.* **2013**, *27*, 221–234. [[CrossRef](#)]
39. Morris, G.M.; Goodsell, D.S.; Halliday, R.S.; Huey, R.; Hart, W.E.; Belew, R.K.; Olson, A.J. Automated docking using a Lamarckian genetic algorithm and an empirical binding free energy function. *J. Comput. Chem.* **1998**, *19*, 1639–1662. [[CrossRef](#)]
40. Dassault Systèmes BIOVIA. *Discovery Studio Modeling Environment*; Dassault Systèmes BIOVIA: San Diego, CA, USA, 2017.
41. Rauf, A.; Akram, M.; Semwal, P.; Mujawah, A.A.H.; Muhammad, N.; Riaz, Z.; Munir, N.; Piotrovsky, D.; Vdovina, I.; Bouyahya, A.; et al. Antispasmodic Potential of Medicinal Plants: A Comprehensive Review. *Oxidative Med. Cell. Longev.* **2021**, *2021*, 4889719. [[CrossRef](#)]
42. Bezerra, M.A.C.; Leal-Cardoso, J.H.; Coelho-de-Souza, A.N.; Criddle, D.N.; Fonteles, M.C. Myorelaxant and antispasmodic effects of the essential oil of *Alpinia speciosa* on rat ileum. *Phytother. Res.* **2000**, *14*, 549–551. [[CrossRef](#)]
43. Tanahashi, Y.; Komori, S.; Matsuyama, H.; Kitazawa, T.; Unno, T. Functions of Muscarinic Receptor Subtypes in Gastrointestinal Smooth Muscle: A Review of Studies with Receptor-Knockout Mice. *Int. J. Mol. Sci.* **2021**, *22*, 926. [[CrossRef](#)]
44. Caulfield, M.; Birdsall, N. International Union of Pharmacology. XVII. Classification of muscarinic acetylcholine receptors. *Pharmacol. Rev.* **1998**, *50*, 279–290.
45. Caulfield, M.P. Muscarinic receptors—characterization, coupling and function. *Pharmacol. Ther.* **1993**, *58*, 319–379. [[CrossRef](#)]
46. Sol, I.; Yang, D.K.; Kim, H.J.; Min, K.W.; Kang, T.M.; Kim, S.J.; Kim, K.W.; Park, K.H.; Jeon, J.H.; Choi, K.H.; et al. Five subtypes of muscarinic receptors are expressed in gastric smooth muscles of guinea pig. *Exp. Mol. Med.* **2003**, *35*, 46–52.
47. Bolton, T.B.; Prestwich, S.A.; Zholos, A.V.; Gordienko, D.V. Excitation-contraction coupling in gastrointestinal and other smooth muscles. *Annu. Rev. Physiol.* **1999**, *61*, 85–115. [[CrossRef](#)]
48. Ehlert, F.J.; Ostrom, R.S.; Sawyer, G.W. Subtypes of the muscarinic receptor in smooth muscle. *Life Sci.* **1997**, *61*, 1729–1740. [[CrossRef](#)]
49. Sawyer, G.W.; Ehlert, F.J. Muscarinic M-3 receptor inactivation reveals a pertussis toxin-sensitive contractile response in the guinea pig colon: Evidence for M-2/M-3 receptor interactions. *J. Pharmacol. Exp. Ther.* **1999**, *289*, 464–476. [[PubMed](#)]
50. Zholos, A.V.; Bolton, T.B. Muscarinic receptor subtypes controlling the cationic current in guinea-pig ileal smooth muscle. *Br. J. Pharmacol.* **1997**, *122*, 885–893. [[CrossRef](#)] [[PubMed](#)]

51. Komori, S.; Unno, T.; Nakayama, T.; Ohashi, H. M2 and M3 muscarinic receptors couple, respectively, with activation of nonselective cationic channels and potassium channels in intestinal smooth muscle cells. *Jpn. J. Pharmacol.* **1998**, *76*, 213–218. [[CrossRef](#)]
52. Pucovsky, V.; Zholos, A.V.; Bolton, T.B. Muscarinic cation current and suppression of Ca²⁺ current in guinea pig ileal smooth muscle cells. *Eur. J. Pharmacol.* **1998**, *346*, 323–330. [[CrossRef](#)] [[PubMed](#)]
53. Amato, A.; Serio, R.; Mulè, F. Involvement of cholinergic nicotinic receptors in the menthol-induced gastric relaxation. *Eur. J. Pharmacol.* **2014**, *745*, 129–134. [[CrossRef](#)]
54. Sadraei, H.; Asghari, G.; Kasiri, F. Comparison of antispasmodic effects of *Dracocephalum kotschyi* essential oil, limonene and α -terpineol. *Res. Pharm. Sci.* **2015**, *10*, 109–116.
55. Lozon, Y.; Sultan, A.; Lansdell, S.J.; Prytkova, T.; Sadek, B.; Yang, K.-H.S.; Howarth, F.C.; Millar, N.S.; Oz, M. Inhibition of human α 7 nicotinic acetylcholine receptors by cyclic monoterpene carveol. *Eur. J. Pharmacol.* **2016**, *776*, 44–51. [[CrossRef](#)]
56. Ratz, P.H.; Berg, K.M.; Urban, N.H.; Miner, A.S. Regulation of Smooth Muscle Calcium Sensitivity: KCl as a Calcium-Sensitizing Stimulus. *Am. J. Physiol.-Cell Physiol.* **2005**, *288*, 769–783. [[CrossRef](#)]
57. Mori, M.X.; Itsuki, K.; Hase, H.; Sawamura, S.; Kurokawa, T.; Mori, Y.; Inoue, R. Dynamics of receptor-operated Ca²⁺ currents through TRPC channels controlled via the PI(4,5)P₂-PLC signaling pathway. *Front. Pharmacol.* **2015**, *6*, 22–26. [[CrossRef](#)]
58. Hu, G.Y.; Peng, C.; Xie, X.F.; Xiong, L.; Zhang, S.Y.; Cao, X.Y. Patchouli alcohol isolated from Pogostemon cablin mediates endothelium-independent vasorelaxation by blockade of Ca²⁺ channels in rat isolated thoracic aorta. *J. Ethnopharmacol.* **2018**, *220*, 188–196. [[CrossRef](#)]
59. Chen, F.; Xu, Y.; Wang, J.; Yang, X.; Cao, H.; Huang, P. Relaxation Effect of Patchouli Alcohol in Rat Corpus Cavernous and Its Underlying Mechanisms. *Evid. Based Complement. Altern. Med.* **2020**, *2020*, 3109069. [[CrossRef](#)]
60. Mathela, C.S.; Chanotiya, C.S.; Sammal, S.S.; Pant, A.K.; Pandey, S. Compositional diversity of terpenoids in Evidence-Based Complementary and Alternative Medicine the Himalayans *Valeriana* genera. *Chem. Biodivers.* **2005**, *2*, 1174–1182. [[CrossRef](#)]
61. Bashir, S.; Memon, R.; Gilani, A.H. Antispasmodic and Antidiarrheal Activities of *Valeriana hardwickii* Wall. Rhizome are Putatively Mediated through Calcium Channel Blockade. *Evid. Based Complement. Altern. Med.* **2011**, *2011*, 304960. [[CrossRef](#)]
62. Vogalis, F. Potassium channels in gastrointestinal smooth muscle. *J. Auton. Pharmacol.* **2000**, *20*, 207–219. [[CrossRef](#)]
63. McHugh, D.; Beech, D.J. Inhibition of delayed rectifier K(+) current by levcromakalim in single intestinal smooth muscle cells: Effects of cations and dependence on K(+) flux. *Br. J. Pharmacol.* **1995**, *114*, 391–399. [[CrossRef](#)]
64. Cornejo, I.; Villanueva, S.; Burgos, J.; López-Cayuqueo, K.I.; Chambrey, R.; Julio-Kalajzić, F.; Buelvas, N.; Niemeyer, M.I.; Figueiras-Fierro, D.; Brown, P.D.; et al. Tissue Distribution of Kir7.1 Inwardly Rectifying K⁺ Channel Probed in a Knock-in Mouse Expressing a Haemagglutinin-Tagged Protein. *Front. Physiol.* **2018**, *9*, 428. [[CrossRef](#)]
65. Gilani, A.H.; Khan, A.U.; Jabeen, Q.; Subhan, F.; Ghafar, R. Antispasmodic and blood pressure lowering effects of *Valeriana wallichii* are mediated through K⁺ channel activation. *J. Ethnopharmacol.* **2005**, *100*, 347–352. [[CrossRef](#)]
66. Martínez-Pérez, E.F.; Juárez, Z.N.; Hernández, L.R.; Bach, H. Natural Antispasmodics: Source, Stereochemical Configuration, and Biological Activity. *BioMed Res. Int.* **2018**, *2018*, 3819714. [[CrossRef](#)]
67. Xiannenas, I.; Papanephytous, C.P.; Tsalie, E.; Pappas, I.; Triantafillou, E.; Tontis, D.; Kontopidis, G.A. Dietary Supplementation of Benzoic Acid and Essential Oil Compounds Affects Buffering Capacity of the Feeds, Performance of Turkey Poults and Their Antioxidant Status, pH in the Digestive Tract, Intestinal Microbiota and Morphology. *Asian-Australas. J. Anim. Sci.* **2014**, *27*, 225–236. [[CrossRef](#)] [[PubMed](#)]
68. Araruna, M.E.; Serafim, C.; Alves Júnior, E.; Hiruma-Lima, C.; Diniz, M.; Batista, L. Intestinal Anti-Inflammatory Activity of Terpenes in Experimental Models (2010–2020): A Review. *Molecules* **2020**, *25*, 5430. [[CrossRef](#)] [[PubMed](#)]
69. Zheng, Z.; Tang, J.; Hu, Y.; Zhang, W. Role of gut microbiota-derived signals in the regulation of gastrointestinal motility. *Front. Med.* **2022**, *9*, 961703. [[CrossRef](#)] [[PubMed](#)]

Disclaimer/Publisher's Note: The statements, opinions and data contained in all publications are solely those of the individual author(s) and contributor(s) and not of MDPI and/or the editor(s). MDPI and/or the editor(s) disclaim responsibility for any injury to people or property resulting from any ideas, methods, instructions or products referred to in the content.